



Calhoun: The NPS Institutional Archive
DSpace Repository

Theses and Dissertations

1. Thesis and Dissertation Collection, all items

1988

Development of a differential temperature
probe for the measurement of atmospheric
turbulence at all levels

Olmstead, Michael Roy.

Monterey, California. Naval Postgraduate School

<http://hdl.handle.net/10945/23172>

Downloaded from NPS Archive: Calhoun



Calhoun is the Naval Postgraduate School's public access digital repository for research materials and institutional publications created by the NPS community. Calhoun is named for Professor of Mathematics Guy K. Calhoun, NPS's first appointed -- and published -- scholarly author.

Dudley Knox Library / Naval Postgraduate School
411 Dyer Road / 1 University Circle
Monterey, California USA 93943

<http://www.nps.edu/library>

NAVAL POSTGRADUATE SCHOOL

Monterey, California



THESIS

0472

Development of a Differential Temperature Probe for
the Measurement of Atmospheric Turbulence at All
Levels

by

Michael Roy Olmstead

December 1988

Thesis Advisor:

D. L. Walters

Approved for public release: Distribution is unlimited.

Prepared for:

Strategic Defense Initiative Organization
1717 H. Street
Washington, DC 20301

J244344

NAVAL POSTGRADUATE SCHOOL
Monterey, CA 93943

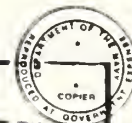
Rear Admiral R. C. Austin
Superintendent

H. Shull
Provost

This thesis prepared in conjunction with research sponsored in part by the Strategic Defense Initiative Organization with funds provided by the Naval Postgraduate School under NPS 61-89-003.

Reproduction of all or part of this report is authorized.

REPORT DOCUMENTATION PAGE



REPORT SECURITY CLASSIFICATION UNCLASSIFIED		1b RESTRICTIVE MARKINGS	
SECURITY CLASSIFICATION AUTHORITY		3 DISTRIBUTION/AVAILABILITY OF REPORT	
DECLASSIFICATION/DOWNGRADING SCHEDULE		Approved for public release: distribution is unlimited.	
PERFORMING ORGANIZATION REPORT NUMBER(S) NPS 61-89-003		5 MONITORING ORGANIZATION REPORT NUMBER(S)	
NAME OF PERFORMING ORGANIZATION Naval Postgraduate School	6b OFFICE SYMBOL (If applicable) 61	7a NAME OF MONITORING ORGANIZATION Strategic Defense Initiative Organization (SDIO/DE)	
ADDRESS (City, State, and ZIP Code) Monterey, California 93943- 5000		7b ADDRESS (City, State, and ZIP Code) 1717 H Street Washington, D.C. 20301	
NAME OF FUNDING / SPONSORING ORGANIZATION Naval Postgraduate School	8b OFFICE SYMBOL (If applicable) 61	9 PROCUREMENT INSTRUMENT IDENTIFICATION NUMBER	
ADDRESS (City, State, and ZIP Code) Monterey, California 93943- 5000		10 SOURCE OF FUNDING NUMBERS	
		PROGRAM ELEMENT NO	PROJECT NO
		TASK NO	WORK UNIT ACCESSION NO
TITLE (Include Security Classification) Development of a Differential Temperature Probe for the Measurement of Atmospheric Turbulence All Levels			
PERSONAL AUTHOR(S) Winstead, Michael R. in conjunction with Donald L. Walters			
TYPE OF REPORT Master's Thesis	13b TIME COVERED FROM _____ TO _____	14 DATE OF REPORT (Year, Month, Day) 1988 December	15 PAGE COUNT 92
SUPPLEMENTARY NOTATION The views expressed in this thesis are those of the author and do not reflect the official policy or position of the Department of Defense or the U.S. Government.			
COSATI CODES		18 SUBJECT TERMS (Continue on reverse if necessary and identify by block number)	
FIELD	GROUP	SUB-GROUP	
		Atmospheric Optics, Atmospheric Turbulence, Temperature Structure Parameter, Acoustic Echosounder, Temperature Probe	
ABSTRACT (Continue on reverse if necessary and identify by block number)			
<p>Fluctuating temperature structures in the atmosphere induce phase perturbations in a propagating laser beam. These turbulent conditions occur throughout the atmosphere and cause the laser beam to spread and alter its centroid. There are several methods to measure the parameters of optical turbulence in the atmosphere, but few that will determine them as a function of altitude at all levels. One method of measuring altitude profiles of turbulence is with a temperature probe launched via a balloon system.</p> <p>This thesis involves the development of a differential temperature probe sensor to measure the temperature fluctuations at all altitudes in the atmosphere. In addition, it investigates the effect of solar heating on the probes in the atmosphere and the subsequent effects on the measurements. A validation of the probe system was made by a comparison</p>			
DISTRIBUTION/AVAILABILITY OF ABSTRACT <input checked="" type="checkbox"/> UNCLASSIFIED/UNLIMITED <input type="checkbox"/> SAME AS RPT <input type="checkbox"/> DTIC USERS		21 ABSTRACT SECURITY CLASSIFICATION UNCLASSIFIED	
NAME OF RESPONSIBLE INDIVIDUAL D. L. Walters		22b TELEPHONE (Include Area Code) (408) 646-2267	22c OFFICE SYMBOL 61We

19. (Continued)

test with an acoustic echosounder developed earlier. In addition to validating the probe system, the absolute C_T^2 analysis of the echosounder was confirmed.

Approved for public release; distribution is unlimited.

Development of a Differential Temperature Probe for
the Measurement of Atmospheric Turbulence at All Levels

by


Michael Roy Olmstead
Lieutenant, United States Navy
B.S., United States Naval Academy, 1981

Submitted in partial fulfillment of the
requirements for the degree of

MASTER OF SCIENCE IN PHYSICS

from the

NAVAL POSTGRADUATE SCHOOL
December 1988



ABSTRACT

Fluctuating temperature structures in the atmosphere induce phase perturbations in a propagating laser beam. These turbulent conditions occur throughout the atmosphere and cause the laser beam to spread and alter its centroid. There are several methods to measure the parameters of optical turbulence in the atmosphere, but few that will determine them as a function of altitude at all levels. One method of measuring altitude profiles of turbulence is with a temperature probe launched via a balloon system.

This thesis involves the development of a differential temperature probe sensor to measure the temperature fluctuations at all altitudes in the atmosphere. In addition, it investigates the effect of solar heating on the probes in the atmosphere and the subsequent effects on the measurements. A validation of the probe system was made by a comparison test with an acoustic echosounder developed earlier. In addition to validating the probe system, the absolute C_T^2 analysis of the echosounder was confirmed.

LIST OF FIGURES

Figure 1. Comparison of LASER Beam Propagating Through Vacuum and Atmosphere, showing r_0	8
Figure 2. Two Sources Showing the Effects of the Isoplanatic Angle	8
Figure 3. Spectrum of Turbulence Over All Scale Lengths	12
Figure 4. Noise and Gain Characteristics of the LT1028 OP AMP.	18
Figure 5. Noise and Gain Characteristics of the LT1057 OP AMP.	18
Figure 6. Schematic Diagram of Differential Amplifier . .	19
Figure 7. Noise Spectrum of Amplifier Circuit	21
Figure 8. Noise Output of Probe System.	23
Figure 9. Photo of Circuit and Thermocouple Probe	23
Figure 10. Schematic of Thermocouple Probe.	26
Figure 11. Response Time Versus Wind Speed of a .00254 cm Copper-Constantan Thermocouple . . .	27
Figure 12. Comparison of AFGL Model and Campbell's Model of Solar Heating of Thermocouple	35
Figure 13. Comparison of Convective Conductance	36
Figure 14. Corrected Comparison of solar heating.	37
Figure 15. Hot Wire Anemometer Effect on Copper Constantan Thermocouples	39
Figure 16. Differences Between the Curves of Figure 15	39
Figure 17. Hot Wire Anemometer Effect on 4 micron Tungsten Wire.	40
Figure 18. Layout of Acoustic Echosounder Device[Ref. 28].	43

Figure 19. Echosounder Trace and C_T^2 Measurement and Probe Measurement During Strong Turbulence . .	45
Figure 20. Echosounder Trace and C_T^2 Measurement and Probe Measurement During Light Turbulence. . .	46
Figure 21. Echosounder Trace and C_T^2 Measurement and Probe Measurement During No Turbulence	47
Figure 22. % Error Induced by a Limiting Outer Scale Length	50
Figure 23. Spatial power spectrum Φ_T of temperature fluctuations versus scaled wave number $\kappa\eta$. Solid curve is actual model; the dashed curve is Tatarski's model.[Ref. 30]	52
Figure 24. Comparison of Data From Acoustic Echosounder and Temperature Probe Before Correction for DC Offset.	53
Figure 25. Comparison of Data From Acoustic Echosounder and Temperature Probe After Correction for DC Offset.	54

I. INTRODUCTION

Atmospheric conditions will cause severe degradation along the optical path of a ground to space weapon or surveillance laser. There are several causes for this degradation, they are 1) absorption and scattering by aerosols such as rain and clouds, 2) distortion by thermal blooming and 3) distortion by atmospheric turbulence [Ref. 1]. Absorption and scattering can be controlled by varying the wavelengths of the laser and having multiple sites to insure at least one has a cloud free line of sight. Thermal blooming is the heating of the medium, through which the laser beam propagates. It is due to absorption of the radiation by molecules and aerosols and the consequent distortion of the beam due to density reductions brought on by the heating. Choosing approximate wavelengths of the laser which have low atmospheric absorption in the atmosphere reduces this effect. Atmospheric turbulence is difficult to deal with since there is no way to avoid it.

The major effect of turbulence on an optical beam is the limitation of the mutual coherence lengths. For example, an average ground to space coherence length for the atmosphere is on the order of 5 cm therefore a ground based laser having

a 4 meter diameter mirror will deliver less than 1/1000 of its original power onto a target. Adaptive optics provides a means for reducing these turbulent effects. It corrects for the effects of turbulence by altering the wavefront characteristics of a beam [Ref. 2] using deformable mirrors or nonlinear optical materials such as Barium Titanate.

Measurements of the turbulence from the surface to an altitude where the turbulence is no longer significant (approximately 30 km.) are needed for several reasons. The most important is to be able to characterize the turbulent profiles of the atmosphere at different locations in order to select the best site for a ground based optical or surveillance system. Each site will have a different turbulence profile since it depends on the local geography as well as the upper atmospheric conditions controlled by general meteorological patterns. Another reason for the measurements is to determine vertical distribution of the turbulence parameters, such as the coherence length, which affect the design of adaptive optics systems, or the signal processing transformations in a surveillance system.

There are several instruments for measuring turbulence parameters, some of which measure the index of refraction structure parameter and others that measure the temperature structure parameter. Some of the methods include analysis of star trails on photographic emulsions [Ref. 3], an

isoplanometer which measures the isoplanatic angle through stellar scintillation [Ref. 4], and a Modulation Transfer Function (MTF) device for determining the coherence length [Ref. 5]. These devices measure important integrated parameters but they cannot measure the vertical profile of turbulence. An acoustic echosounder which is similar in design and construction to a SONAR [Ref. 6], measures a vertical profile but is usually limited to several hundred meters range. Greater vertical resolution occurs at the expense of decreased maximum range.

In order to get a measurement of the vertical profile of turbulence to 20-50 km a device must be able to be launched on a sounding balloon or an aircraft. An example of this type of device is the thermosonde originally designed by GTE Sylvania and revised by the Air Force Weapons Laboratory and Tri-Con Associates Inc. and built and used by the Air Force Geophysics Laboratory [Ref. 7].

This thesis is an attempt to design and build a temperature sensing probe system to measure the vertical profile of the temperature structure parameter which is a measure of the vertical profile of turbulence. Although such systems exist, they are 1) expensive, greater than \$2000 per launch and 2) require extensive calibration. The purpose of this thesis was to develop an inexpensive device (the system cost is approximately \$150 per launch) which is simple to

operate (it is a self-calibrating device). Additionally the effects of solar heating of the probes are investigated.

The results of a comparison with a well developed acoustic echosounder indicates the system will be effective in measuring turbulence in the atmosphere. The studies of the solar heating effects indicate the only source of error due to solar heating would be from the sun/shade effect on the two probes and if that is corrected for, it will be accurate up to 30 km.

II. BACKGROUND

A. TURBULENCE PARAMETERS

Small temperature variations carried by the turbulent velocity field in the atmosphere produce small phase perturbations in an optical plane wave propagating through it. These perturbations randomly distort and convolve the phase of a plane wave. There are three atmospheric parameters which must be determined prior to any attempt made at compensating for these atmospheric distortions. These parameters are the refractive turbulence structure parameter, C_N^2 , the spatial coherence length of the atmosphere, r_0 , and the isoplanatic angle θ_0 .

The most important of these parameters is C_N^2 . Tatarski [Ref. 3] states that one way to deal with a non-stationary problem, which includes all atmospheric parameters, is to define a function in terms of a difference, he then defines the structure function for index of refraction as,

$$D_n(\vec{r}_1, \vec{r}_2) = \langle [N(\vec{r}_2) - N(\vec{r}_1)]^2 \rangle, \quad (1)$$

where $\langle \rangle$ denotes an ensemble average. If we assume the atmosphere to be homogeneous and isotropic over small regions the structure function can be rewritten as,

$$D_N(r) = \langle [N(r_2) - N(r_1)]^2 \rangle, \quad (2)$$

where r is $r_1 - r_2$. By dimensional analysis Kolomogorov [Ref. 3] showed that the structure function has an $r^{2/3}$ dependency. Consequently D_N is proportional to a constant C_N^2 times $r^{2/3}$,

$$D_N = C_N^2 r^{2/3}. \quad (3)$$

C_N^2 is the refractive turbulence structure parameter, a mean-square statistical average of the difference in the index of refraction between two points separated by r_{12} ,

$$C_N^2 = \langle (N_2 - N_1)^2 \rangle / r_{12}^{2/3}. \quad (4)$$

The $r^{2/3}$ normalization extends from an inner scale l_0 , on the order of millimeters, to an outer scale of L_0 , on the order of meters [Ref. 3]. These fluctuations in the index of refraction arise from variations in density caused by temperature fluctuations in the turbulent velocity field.

These density variations in the atmosphere alter the phase of an optical beam being propagated through it. The Optical Transfer Function (OTF) characterizes the integrated phase perturbations of an optical beam. It is a measure of the correlation of the electric fields of the optical beam

perpendicular to the direction of propagation. Although the atmosphere is not homogeneous or isotropic, Tatarski [Ref. 8] postulates the idea of local homogeneity and isotropy, which states that over some region R , comparable to the outer scale length L_0 , we can assume the atmospheric random variables are homogeneous and isotropic. The modulus of the OTF is the atmospheric Modulation Transfer Function (MTF). Fried [Ref. 9] introduces the parameter r_0 to characterize the MTF. It is related to the refractive turbulence structure parameter by,

$$r_0 = 2.1 \left[1.46k^2 \int_0^L C_n^2(z) dz \right]^{-3/5}, \quad (5)$$

where r_0 is the spatial coherence length, k is the wave number ($2\pi/\lambda$), and C_n^2 is the refractive turbulence structure parameter along the optical path of length L [Ref. 5].

The other measure of spatial coherence in the atmosphere is the isoplanatic angle θ_0 . It is similar to r_0 in that it is the dependence of the optical transfer function of a system for different angles to the source. The two parameters r_0 and θ_0 are conjugate pairs. θ_0 looking up is equivalent to r_0 divided by the path length looking down [Ref. 4] and vice versa. A more formal definition is that θ_0 is an angular measure of spatial coherence, it is the limiting angle for which an electromagnetic wave from a source will follow the same optical path length to a receiver.

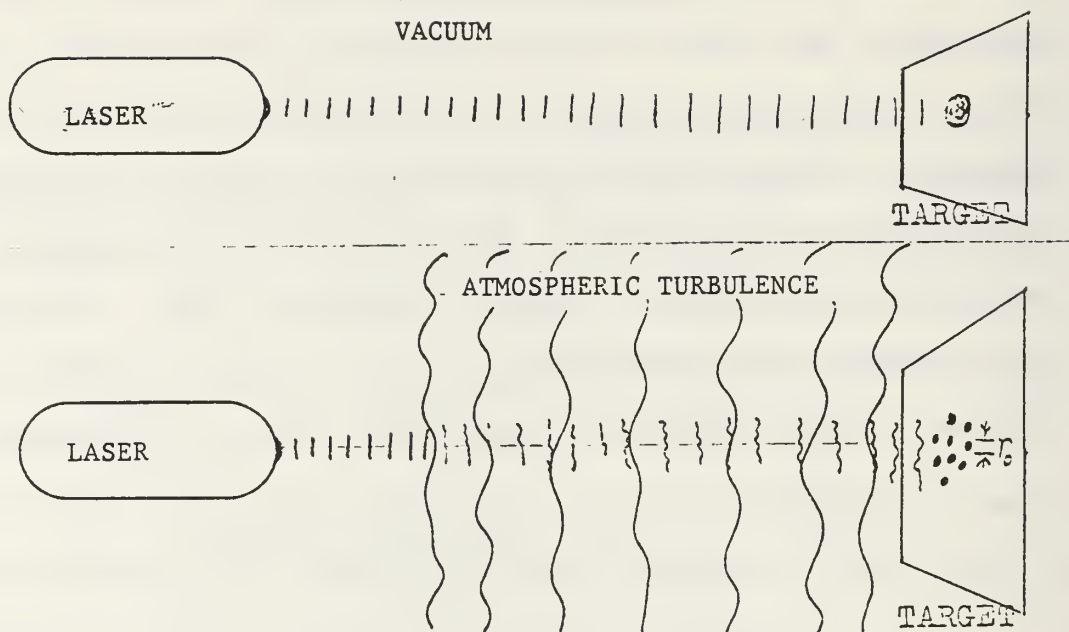


Figure 1. Comparison of LASER Beam Propagating Through Vacuum and Atmosphere, showing r_0 .

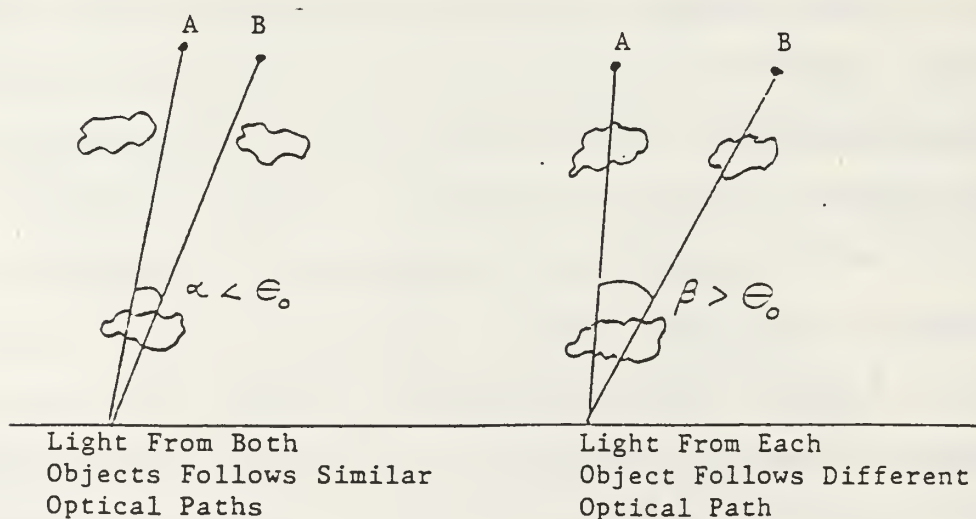


Figure 2. Two Sources Showing the Effects of the Isoplanatic Angle.

If we consider two paths through the turbulence, the isoplanatic angle relates the mutual coherence e^{-1} point of the E field between the two paths. Fried [Ref. 9] expresses the isoplanatic angle's dependence on C_N^2 as,

$$\theta_0 = \left[2.905 k^2 \int_0^L C_N^2(z) z^{5/3} dz \right]^{-3/5}, \quad (6)$$

where z is the altitude. Note the $z^{5/3}$ spherical weighting factor that emphasizes turbulence far from the optical system.

The preceding paragraphs clearly show the importance of the C_N^2 parameter, it not only defines the measure of turbulence, it also determines the spatial coherence r_0 and the isoplanatic angle θ_0 . The problem lies in that high resolution profiles of C_N^2 are difficult to measure, it requires complex detectors and optical imaging systems. Instead we can define a temperature structure parameter C_T^2 similar to C_N^2 where,

$$C_T^2 = \langle (T_2 - T_1)^2 \rangle / r_{12}^{2/3}, \quad (7)$$

which can be measured by several different methods. The fluctuations of the index of refraction are due to fluctuations in the density of the atmosphere and if we can assume that the density fluctuations are due solely to temperature fluctuations, then C_T^2 is related to C_N^2 by,

$$C_n^2 = \left[\frac{79 \times 10^{-6} P}{T^2} \right] C_T^2, \quad (8)$$

where P is the atmospheric pressure in millibars and T is the atmospheric temperature in Kelvins [Ref. 10]. The assumption that index of refraction fluctuations are due only to temperature fluctuations and that humidity fluctuations are insignificant, is valid when the Bowen Ratio B (ratio of sensible heat flux to latent heat flux) is greater than 0.3 [Refs. 11,12]. Below this value, humidity fluctuations are significant.

B. SCALE LENGTHS

In Kolomogorov's definition of the structure function he assumed local homogeneity over a region bounded by the inner and outer scale lengths l_0 and L_0 . These scale lengths vary from hundreds of meters at the outer scale lengths down to millimeters for the inner scale lengths [Ref. 13]. The outer scale length is the size of the turbulent fluctuations at the onset, while at the inner scale viscosity dissipates the energy of turbulence as heat. Kolomogorov called the region between l_0 and L_0 the inertial subrange and as long as the distance r , in Equations (4) and (7), is within this inertial subrange these equations are valid. Kolomogorov expressed the power spectral density of the turbulence in this region by,

$$\phi(K) = 0.033 C_n^2 K^{-11/3}, \quad (9)$$

where $2\pi L_0^{-1} \ll K \ll 2\pi l_0^{-1}$. Von Karman took this definition further to include the ranges for eddy sizes greater than L_0 ,

$$\phi_n(K) = \frac{\Gamma(11/6)}{\Gamma(1/3)} \frac{\pi^{-9/2}}{8} \langle \delta_n^2 \rangle L_0^3 \left[1 + \frac{K^2}{K_0^2} \right]^{-11/6}, \quad (10)$$

where $K_0 = 2\pi L_0^{-1}$ and $\langle \delta_n^2 \rangle$ is the variance of the refractivity fluctuations and is related to C_n^2 by,

$$C_n^2 \approx 1.9 \langle \delta_n^2 \rangle K_0^{2/3}, \quad (11)$$

[Ref. 10]. Figure 3 shows the spectrum of turbulence for all scale lengths, the inertial subrange shows Kolomogorov's linear description of turbulence while in the regions above $2\pi l_0^{-1}$ viscosity effects dominate and below $2\pi L_0^{-1}$ Von Karman's spectrum defines the turbulence [Ref. 14].

It is important to understand the effects of the turbulence spectrum in all three regions because of the errors introduced due to the lack of correlation in the regions above and below the inertial subrange. Care must be taken in choosing the correct value of r to cover the scale lengths inside the inertial subrange. Additionally the temporal frequency of the turbulent fluctuations is related to the wave

number K and the wind speed moving the turbulence past the probes. Therefore to measure the thin transition layers in the atmosphere accurately [Ref. 15] the errors due to various scale sizes must be determined. These calculations will be carried out in Chapter 4.

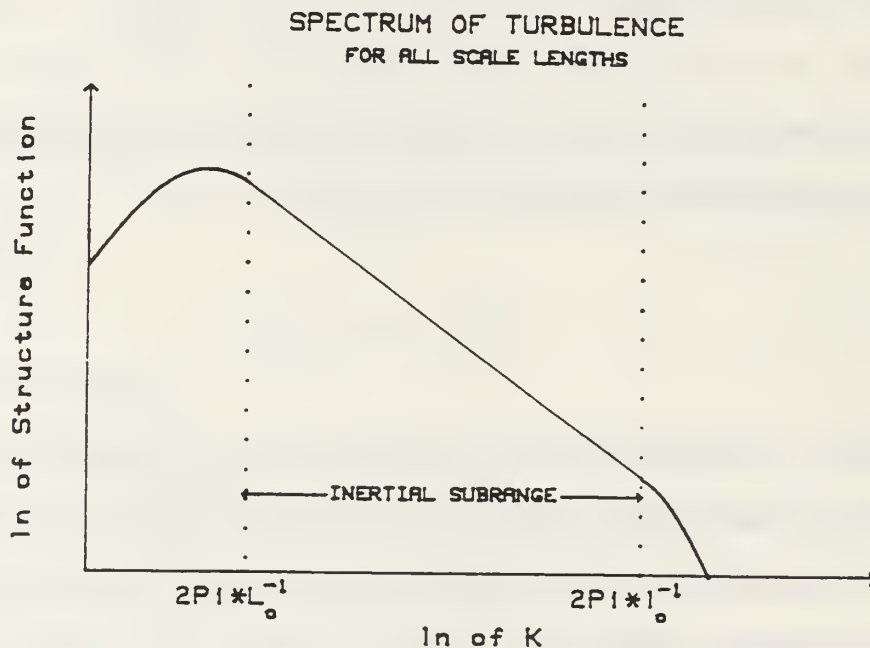


Figure 3. Spectrum of Turbulence Over All Scale Lengths.

C. SYSTEM REQUIREMENTS

A fast response time temperature probe attached to a sounding balloon system can measure the vertical profile of the temperature structure parameter. The design of the temperature probe system provides a simple, low cost method

that is capable of resolving the thin stratified layers of a stable atmosphere and determining the temperature gradient, thickness, and turbulence of these layers. In designing the system the key points of consideration were 1) what type of probe geometry and thereby what type of circuitry and 2) what type of temperature sensing element to use.

The probe system could use a differential measurement or a single point probe. The advantage of the single point probe is that it can measure C_T^2 from either the variance of the data, knowing the balloon ascent rate, or by analyzing the power spectral density. However, this would require a high data rate (several samples per second), which the radiosonde systems used do not have. Although a differential system would not have as high a vertical resolution it has the advantage of providing partially reduced data which relaxes the need for a high data rate. Therefore a differential system greatly simplifies the telemetry needed for the system at the expense of more complexity in the sensor itself. The resolution for the system would still be satisfactory, about 2 meters of vertical resolution for a balloon with an ascent rate of 2 meters per second.

There are several different choices for the probes. They can be made from resistance wires, thermistors, or thermocouples. The resistance wire is simply a fine wire, such as platinum or tungsten, with a known resistance as a function

of temperature. The problem with a resistance wire for this application is that it requires some means of self-calibration due to its dependence on Ohm's law and temperature. A thermistor is a small semiconductor device which changes its resistance as a function of temperature. It has a larger change in resistance vs. temperature than a metal wire, although it is non-linear. However, thermistors are large compared to a fine wire, having a larger thermal mass than a probe made from a fine wire, which increases the response time and the susceptibility to solar heating of the device. Additionally, both the thermistor and the resistance wire require a current source which not only increases the complexity of the circuit but also introduces a self heating factor. A thermocouple consists of two fine wires made of dissimilar metals welded together, which produces a voltage difference proportional to the temperature. For an in-depth discussion of thermocouples and the thermoelectric effect, see Refs. 16 and 17. Commercially available thermocouples can be made of very fine wire (down to $12.5\ \mu\text{m}$) thereby reducing the thermal mass and producing a faster response time. A disadvantage of a thermocouple is that the response to temperature is small, typically $40\ \mu\text{V}/^\circ\text{K}$. This places severe requirements on low noise signal processing. An operational requirement for this type of device would be the knowledge of the mean atmospheric temperature to calculate the Seebeck

Coefficient, which is the derivative of the thermal emf with respect to the temperature. Since the rawinsonde system used with the probe provides this data, it is easily accomplished. Small temperature changes of 1° C or less, are expected from the two probes in a differential system. This produces a negligible change in the Seebeck coefficient therefore no calibration of this type of device is needed, other than knowing the gains of the electronic amplifiers.

III. SYSTEM DESIGN AND DEVELOPMENT

A. AMPLIFIER CIRCUIT

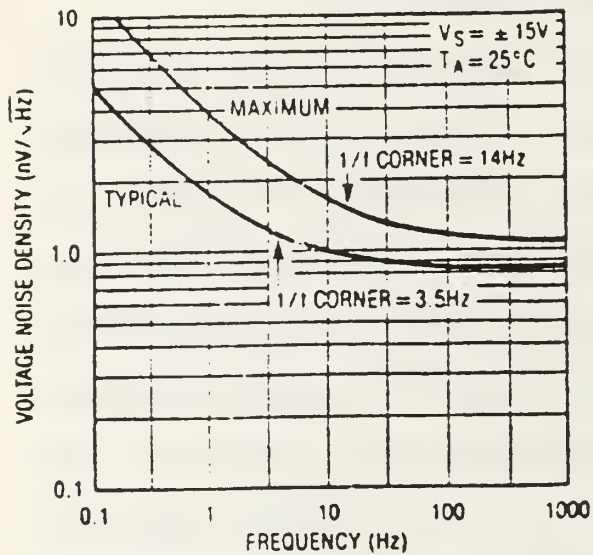
The probe system consists of a pair of thermocouples connected in series and held rigidly 1 meter apart by an aluminum tube. An amplifier circuit requires high voltage gain and very low noise to be able to discriminate the signal from the background due to the low voltage produced by thermocouples (on the order of μ volts per degree). It also requires an analog root mean square device to calculate $\langle(T_2 - T_1)^2\rangle$.

Since the purpose of the system is to measure temperature differences on the order of hundredths and thousandths of a degree and the thermocouple output voltage is about 40 microvolts per degree C the circuit must have a very high gain with ultra low self noise. Therefore the circuit must be carefully designed and built to reduce any sources of noise wherever possible, by methods such as matching resistor values as exact as possible and placing them as close as possible to each other to reduce the thermal drift. Other examples include thermal insulation for the entire circuit and RF shielding for the circuit as well as the probe. The most critical component

of the circuit is the ultra low noise, precision, high speed op amps which have voltage noises less than those of 50 ohm resistors.

The circuit (designed by Prof. Don Walters and fabricated by Dale Galarowicz) is a low noise, wide bandwidth Instrumentation amplifier. Three operational amplifiers produce a gain of 10,000 and a combination low and high pass filter with a gain of 5 producing a total voltage gain of 50,000. The circuit contains two Linear Technologies LT1028 ultra low noise precision high speed op amps in the instrumentation amplifier portion of the circuit. These op amps have a gain bandwidth product of 75 MHz and a self noise of $0.85 \text{ nV/Hz}^{1/2}$ at the frequencies desired. Figure 4 shows the noise and frequency characteristics of this op amp. The filter for the circuit uses an LT1057 op amp whose noise and frequency response characteristics are shown in Figure 5. Based on the frequency response curves in Figures 4 and 5 [Ref. 18] and the high pass filter the circuit has a frequency response from 0.16 Hz to 200 Hz. The other major component of the circuit is an Analog Devices AD637 high precision, wide band RMS-DC converter. It has a bandwidth of 600KHz at 100mV RMS and an averaging time constant of 25 msec/micro F. The entire circuit is powered by two 9 volt dry cells. Figure 6 is a complete schematic diagram of the circuit.

Voltage Noise vs Frequency



Voltage Gain vs Frequency

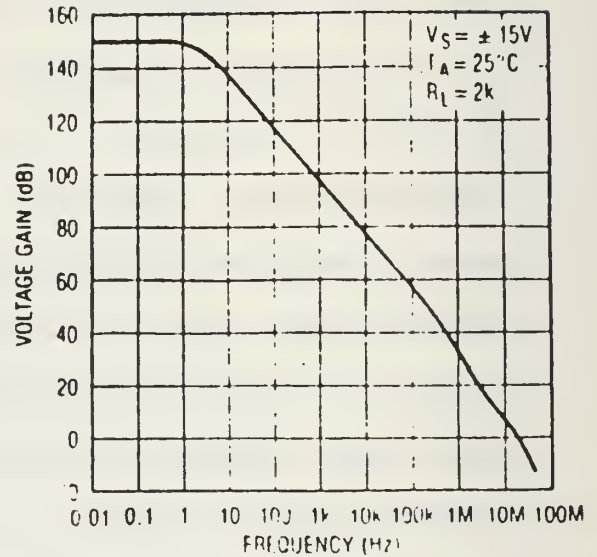


Figure 4. Noise and Gain Characteristics of the LT1028 OP AMP.

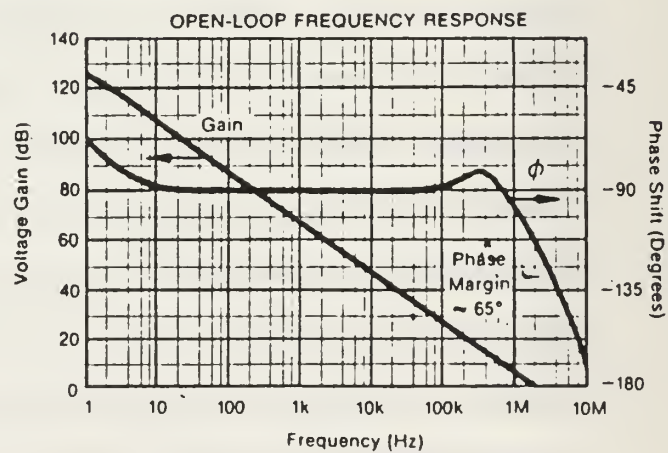
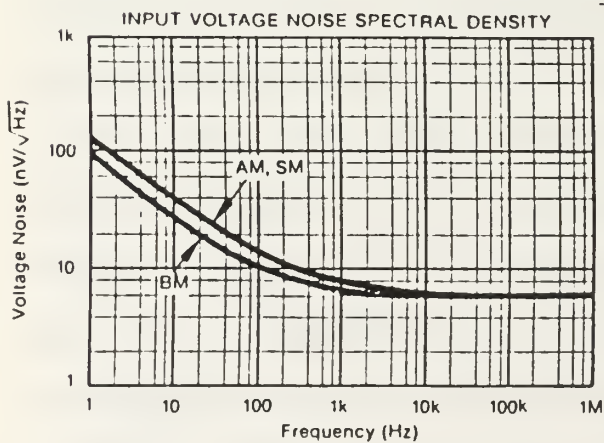
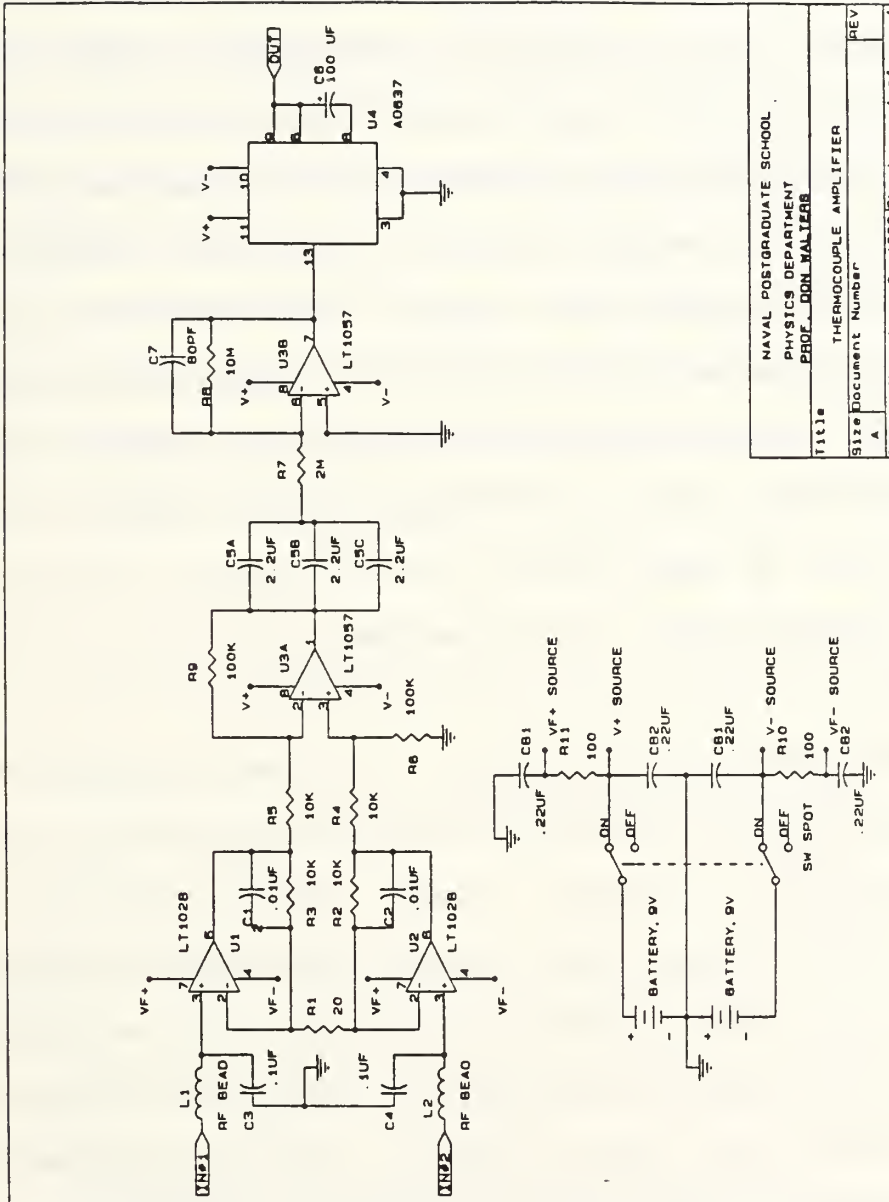


Figure 5. Noise and Gain Characteristics of the LT1057 OP AMP.



NAVAL POSTGRADUATE SCHOOL		
PHYSICS DEPARTMENT		
PROF. DON WALTERS		
Title: THERMOCOUPLE AMPLIFIER		
Size	Document Number	REV
A		
Date	November 9, 1998	Sheet 1 of 1

Figure 6. Schematic Diagram of Differential Amplifier.

The circuit has to be well shielded against RF interference due to the high gain of the circuit and the fact it will be operated in the atmosphere where it is highly susceptible to all types of RF signals. Additionally the thermocouple wires must be stretched out over a distance of 1 meter and will act as an antenna. The aluminum tube shields them from RFI except at the two endpoints, greatly reducing extraneous signals. The circuit is inclosed in a styrofoam casing, to reduce thermal gradients across the circuit, which is then covered in aluminum foil. The circuit itself has ferrite beads and an LC filter, at the inputs, to further shield the op amps from RFI and the entire circuit is built on a ground plane which has been grounded with the foil shield.

The result of the aluminum foil and styrofoam shielding and use of ultra low noise op amps is an amplifier capable of measuring the extremely small voltages produced by the thermocouple probes. The circuit was tested in the anechoic chamber in the basement of Spanagel Hall to minimize any temperature fluctuations and then measurements of the circuits self noise were taken. Figure 7 shows the noise spectrum measured by a Hewlett Packard HP3561A Dynamic Signal Analyzer. The large noise spike below 1 Hz is due to $1/f$ or flicker noise which occurs in all amplifiers, due in large part to surface leakage of transistors [Ref. 19]. Although the noise

normally occurs at frequencies up to 100Hz it has been reduced by the use of a high pass filter. The noise spike at 60Hz is due to AC powered equipment operating in the anechoic chamber. This noise should vanish when the system is used in the field, since it is powered by DC batteries, as long as care is taken to insure it is not near a large AC power source. The plot clearly shows the self noise output of the circuit is well below 100 microVolts/Hz^{1/2} in the frequencies of interest. Since the circuit gain is 50,000 and the Seebeck coefficient is on the order of 40 microVolts per degree this translates into a noise induced measurement of less than 0.00005°C/Hz^{1/2}.

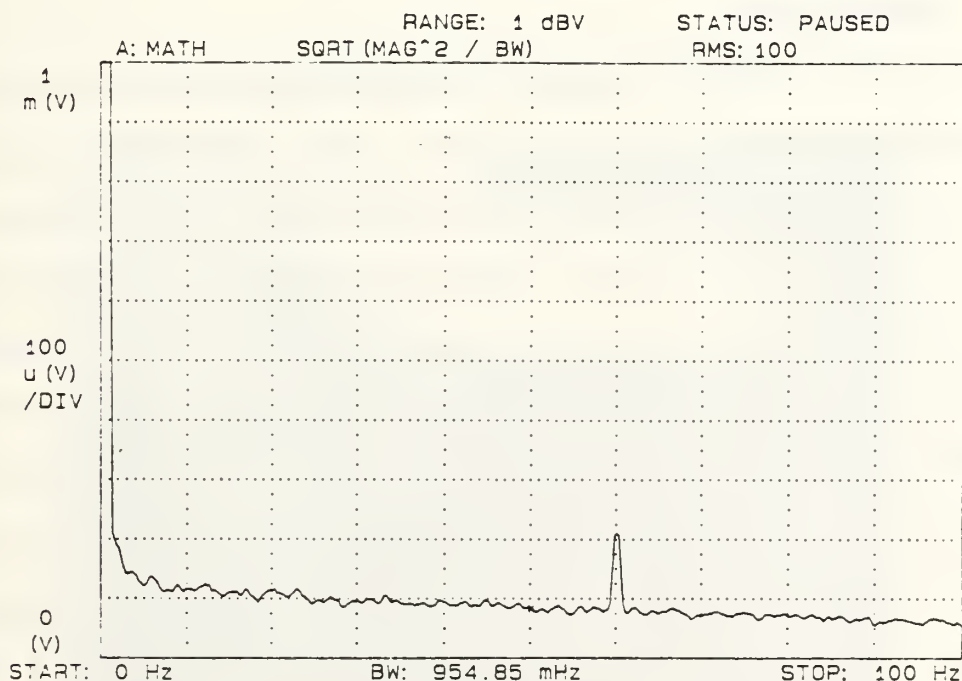


Figure 7. Noise Spectrum of Amplifier Circuit.

The entire system was set-up and run in the anechoic chamber with caps on the exposed thermocouples to further reduce the signal. After running for about 2 hours to let all air currents in the chamber settle, the system produced the results shown in Figure 8. This shows the noise produced by the circuit introduced an error corresponding to a C_T^2 of less than 10^{-6} , which is two orders of magnitude lower than the lowest C_T^2 needed for a usable probe system. These results indicate the circuit self noise is well below that which would have a degrading effect on the results.

The entire circuit package measures 3" X 3" X 3" and weighs less than six ounces.

B. THERMOCOUPLE

In 1821 Thomas Seebeck discovered that two wires of dissimilar metals joined at one end and heated produce a voltage difference across the open ends. This voltage is a function of the junction temperature and the composition of the two metals. Since that time, many different thermocouple types have been produced based on the combination of the two different metals used and having different thermoelectric and physical properties. The requirements for the system included use in the atmosphere from the surface to 20 km, therefore the temperatures vary from 30° C to -30° C with as large a Seebeck coefficient as possible. The Seebeck coefficient is the slope

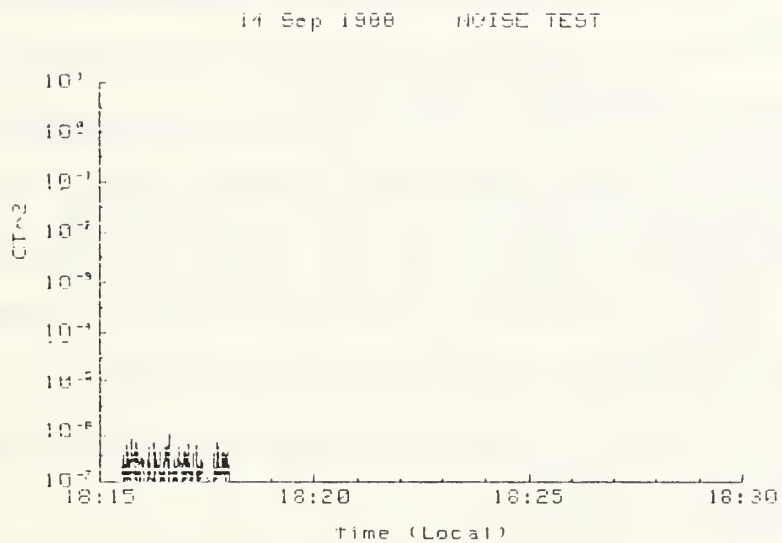


Figure 8. Noise Output of Probe System.

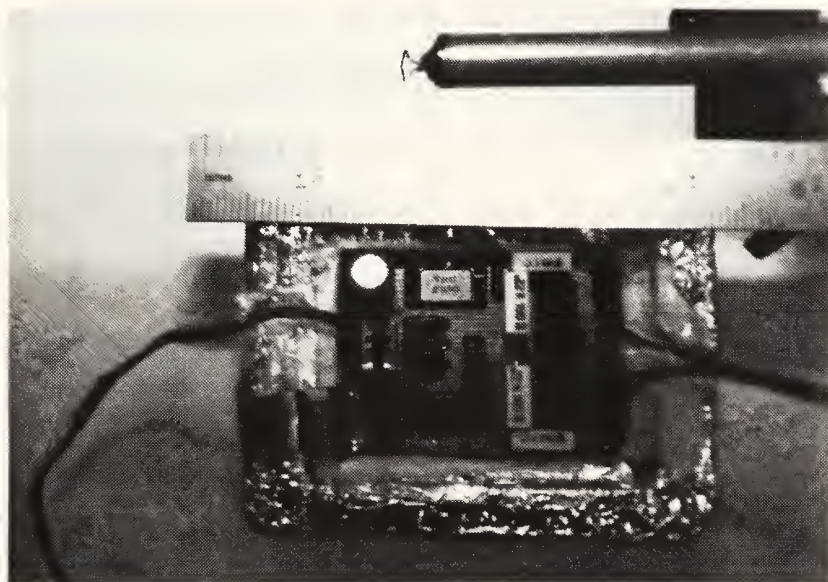


Figure 9. Photo of Circuit and Thermocouple Probe

of the voltage versus temperature curve at a given temperature. Based on these requirements the T type or Copper-Constantan thermocouple was selected. An alternative choice would be the E type or Chromel-Constantan thermocouple.

The Copper-Constantan thermocouple is composed of a copper wire and a 55% copper 45% nickel wire. It has a temperature range of -200°C to 350°C and is suitable for applications where moisture is present. Table 1 shows the thermoelectric voltages referenced to 0°C for a Copper-Constantan thermocouple based on the National Bureau of Standards reference tables.

Table 1 shows that the Seebeck coefficient, which is the unit difference in voltage for each temperature change, is not linear over the entire temperature range. To determine the Seebeck coefficient, dV/dt , valid over the entire temperature range desired, the data over the temperature range desired from Table 1 was plotted and then a polynomial regression was performed to find the equation of the curve. The derivative of the curve was taken to find the Seebeck coefficient. A fifth order polynomial fits the data from -100°C to 30°C . The Seebeck Coefficient for a Copper-Constantan thermocouple is,

$$\begin{aligned} dV/dt = & 3.8707 \times 10^{-2} + 8.5348 \times 10^{-5}t - 3.3135 \times 10^{-7}t^2 \\ & - 2.77432 \times 10^{-9}t^3 - 1.253 \times 10^{-11}t^4, \end{aligned} \quad (12)$$

Table 1

VOLTAGES FOR A TYPE T THERMOCOUPLE

DEG C	0	1	2	3	4	5	6	7	8	9	10	DEG C
THERMOELECTRIC VOLTAGE IN ABSOLUTE MILL VOLTS												
-270	-6.238											-270
-260	-6.232	-6.236	-6.239	-6.242	-6.245	-6.248	-6.251	-6.253	-6.255	-6.256	-6.258	-260
-250	-6.181	-6.187	-6.193	-6.198	-6.204	-6.209	-6.214	-6.219	-6.224	-6.228	-6.232	-250
-240	-6.105	-6.114	-6.122	-6.130	-6.138	-6.146	-6.153	-6.160	-6.167	-6.174	-6.181	-240
-230	-6.007	-6.018	-6.028	-6.039	-6.049	-6.059	-6.068	-6.078	-6.087	-6.096	-6.105	-230
-220	-5.889	-5.901	-5.914	-5.926	-5.938	-5.950	-5.962	-5.973	-5.985	-5.996	-6.007	-220
-210	-5.753	-5.767	-5.782	-5.795	-5.809	-5.823	-5.836	-5.850	-5.863	-5.876	-5.889	-210
-200	-5.603	-5.619	-5.634	-5.650	-5.665	-5.680	-5.695	-5.710	-5.724	-5.739	-5.753	-200
-190	-5.439	-5.456	-5.473	-5.489	-5.506	-5.522	-5.539	-5.555	-5.571	-5.587	-5.603	-190
-180	-5.261	-5.279	-5.297	-5.315	-5.333	-5.351	-5.369	-5.387	-5.404	-5.421	-5.439	-180
-170	-5.069	-5.089	-5.109	-5.128	-5.147	-5.167	-5.186	-5.205	-5.223	-5.242	-5.261	-170
-160	-4.865	-4.886	-4.907	-4.928	-4.948	-4.969	-4.989	-5.010	-5.030	-5.050	-5.069	-160
-150	-4.648	-4.670	-4.693	-4.715	-4.737	-4.758	-4.780	-4.801	-4.823	-4.844	-4.865	-150
-140	-4.419	-4.442	-4.466	-4.489	-4.512	-4.535	-4.558	-4.581	-4.603	-4.626	-4.648	-140
-130	-4.177	-4.202	-4.226	-4.251	-4.275	-4.299	-4.323	-4.347	-4.371	-4.395	-4.419	-130
-120	-3.923	-3.949	-3.974	-4.000	-4.026	-4.051	-4.077	-4.102	-4.127	-4.152	-4.177	-120
-110	-3.656	-3.684	-3.711	-3.737	-3.764	-3.791	-3.818	-3.844	-3.870	-3.897	-3.923	-110
-100	-3.378	-3.407	-3.435	-3.463	-3.491	-3.519	-3.547	-3.574	-3.602	-3.629	-3.656	-100
-90	-3.089	-3.118	-3.147	-3.177	-3.206	-3.235	-3.264	-3.293	-3.321	-3.350	-3.378	-90
-80	-2.788	-2.818	-2.849	-2.879	-2.909	-2.939	-2.970	-2.999	-3.029	-3.059	-3.089	-80
-70	-2.475	-2.507	-2.539	-2.570	-2.602	-2.633	-2.664	-2.695	-2.726	-2.757	-2.788	-70
-60	-2.152	-2.185	-2.218	-2.250	-2.283	-2.315	-2.348	-2.380	-2.412	-2.444	-2.475	-60
-50	-1.819	-1.853	-1.886	-1.920	-1.953	-1.987	-2.020	-2.053	-2.087	-2.120	-2.152	-50
-40	-1.475	-1.510	-1.544	-1.579	-1.614	-1.648	-1.682	-1.717	-1.751	-1.785	-1.819	-40
-30	-1.121	-1.157	-1.192	-1.228	-1.263	-1.299	-1.334	-1.370	-1.405	-1.440	-1.475	-30
-20	-0.757	-0.794	-0.830	-0.867	-0.903	-0.940	-0.976	-1.013	-1.049	-1.085	-1.121	-20
-10	-0.383	-0.421	-0.458	-0.496	-0.534	-0.571	-0.608	-0.646	-0.683	-0.720	-0.757	-10
0	0.000	-0.039	-0.077	-0.116	-0.154	-0.193	-0.231	-0.269	-0.307	-0.345	-0.383	0
DEG C	0	1	2	3	4	5	6	7	8	9	10	DEG C
0	0.000	0.039	0.078	0.117	0.156	0.195	0.234	0.273	0.312	0.351	0.391	0
10	0.391	0.430	0.470	0.510	0.549	0.589	0.629	0.669	0.709	0.749	0.789	10
20	0.789	0.830	0.870	0.911	0.951	0.992	1.032	1.073	1.114	1.155	1.196	20
30	1.196	1.237	1.279	1.320	1.361	1.403	1.444	1.486	1.528	1.569	1.611	30
40	1.611	1.653	1.695	1.738	1.780	1.822	1.865	1.907	1.950	1.992	2.035	40
50	2.035	2.078	2.121	2.164	2.207	2.250	2.294	2.337	2.380	2.424	2.467	50
60	2.467	2.511	2.555	2.599	2.643	2.687	2.731	2.775	2.819	2.864	2.908	60
70	2.908	2.953	2.997	3.042	3.087	3.131	3.176	3.221	3.266	3.312	3.357	70
80	3.357	3.402	3.447	3.493	3.538	3.584	3.630	3.676	3.721	3.767	3.813	80
90	3.813	3.859	3.906	3.952	3.998	4.044	4.091	4.137	4.184	4.231	4.277	90
100	4.277	4.324	4.371	4.418	4.465	4.512	4.559	4.607	4.654	4.701	4.749	100
110	4.749	4.796	4.844	4.891	4.939	4.987	5.035	5.083	5.131	5.179	5.227	110
120	5.227	5.275	5.324	5.372	5.420	5.469	5.517	5.566	5.615	5.663	5.712	120
130	5.712	5.761	5.810	5.859	5.908	5.957	6.007	6.056	6.105	6.155	6.204	130
140	6.204	6.254	6.303	6.353	6.403	6.452	6.502	6.552	6.602	6.652	6.702	140
150	6.702	6.753	6.803	6.853	6.903	6.954	7.004	7.055	7.106	7.156	7.207	150
160	7.207	7.258	7.309	7.360	7.411	7.462	7.513	7.564	7.615	7.666	7.718	160
170	7.718	7.769	7.821	7.872	7.924	7.975	8.027	8.079	8.131	8.183	8.235	170
180	8.235	8.287	8.339	8.391	8.443	8.495	8.548	8.600	8.652	8.705	8.757	180
190	8.757	8.810	8.863	8.915	8.968	9.021	9.074	9.127	9.180	9.233	9.286	190
200	9.286	9.339	9.392	9.446	9.499	9.553	9.606	9.659	9.713	9.767	9.820	200
210	9.820	9.874	9.928	9.982	10.036	10.090	10.144	10.198	10.252	10.306	10.360	210
220	10.360	10.414	10.468	10.523	10.578	10.632	10.687	10.741	10.796	10.851	10.905	220
230	10.905	10.960	11.015	11.070	11.125	11.180	11.235	11.290	11.345	11.401	11.456	230
240	11.456	11.511	11.566	11.622	11.677	11.733	11.788	11.844	11.900	11.956	12.011	240
250	12.011	12.067	12.123	12.179	12.235	12.291	12.347	12.403	12.459	12.515	12.572	250
260	12.572	12.628	12.684	12.741	12.797	12.854	12.910	12.967	13.024	13.080	13.137	260
270	13.137	13.194	13.251	13.307	13.364	13.421	13.478	13.535	13.592	13.650	13.707	270
280	13.707	13.764	13.821	13.879	13.936	13.993	14.051	14.108	14.166	14.223	14.281	280
290	14.281	14.339	14.396	14.454	14.512	14.570	14.628	14.686	14.744	14.802	14.860	290
300	14.860	14.918	14.976	15.034	15.092	15.151	15.209	15.267	15.326	15.384	15.443	300
310	15.443	15.501	15.560	15.619	15.677	15.736	15.795	15.853	15.912	15.971	16.030	310
320	16.030	16.089	16.148	16.207	16.266	16.325	16.384	16.444	16.503	16.562	16.621	320
330	16.621	16.681	16.740	16.800	16.859	16.919	16.978	17.038	17.097	17.157	17.217	330
340	17.217	17.277	17.336	17.396	17.456	17.516	17.576	17.636	17.696	17.756	17.816	340
350	17.816	17.877	17.937	17.997	18.057	18.118	18.178	18.238	18.299	18.359	18.420	350
360	18.420	18.480	18.541	18.602	18.662	18.723	18.784	18.845	18.905	18.966	19.027	360
370	19.027	19.088	19.149	19.210	19.271	19.332	19.393	19.455	19.516	19.577	19.638	370
380	19.638	19.699	19.761	19.822	19.883	19.945	20.006	20.068	20.129	20.191	20.252	380
390	20.252	20.314	20.376	20.437	20.499	20.560	20.622	20.684	20.746	20.807	20.869	390
400	20.869											400
DEG C	0	1	2	3	4	5	6	7	8	9	10	DEG C

where t is in $^{\circ}\text{C}$ and V is in millivolts. The temperature difference measured by the probe, is the output voltage divided by the circuit gain and divided by dV/dt determined at the specific temperature. For a 1° change in air temperature the average change in dV/dt is less than 0.2 microVolts per degree C or less than 0.5% change in dV/dt .

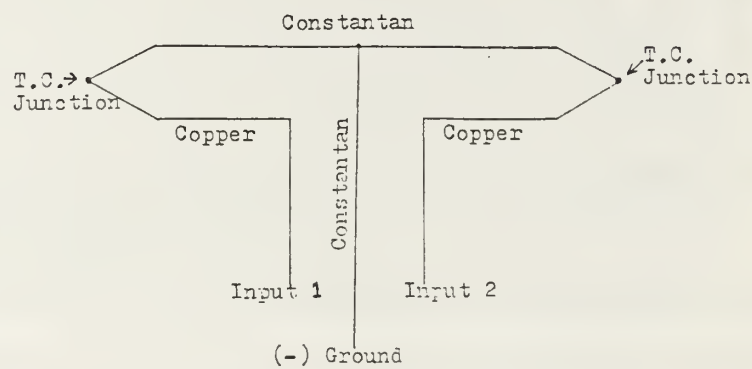


Figure 10. Schematic of Thermocouple Probe.

The probe consists of two 0.00254 cm diameter Copper-Constantan thermocouples held rigidly 1 meter apart by an aluminum tube. This wire has a resistance of 998.3 ohms per double meter and the circuit requires a low input impedance, therefore it is necessary to cut the fine thermocouple wire short and solder larger wires to them to run the distance between the thermocouples and the circuit input. Copper-Constantan wires 0.0254 cm in diameter were used which have a resistance of 9.983 ohms per double meter. It is essential to solder the copper to copper and constantan to constantan

to insure no other thermocouple junctions are formed which could cancel any voltage signal generated. The resulting probe yields an input resistance of 30 ohms.

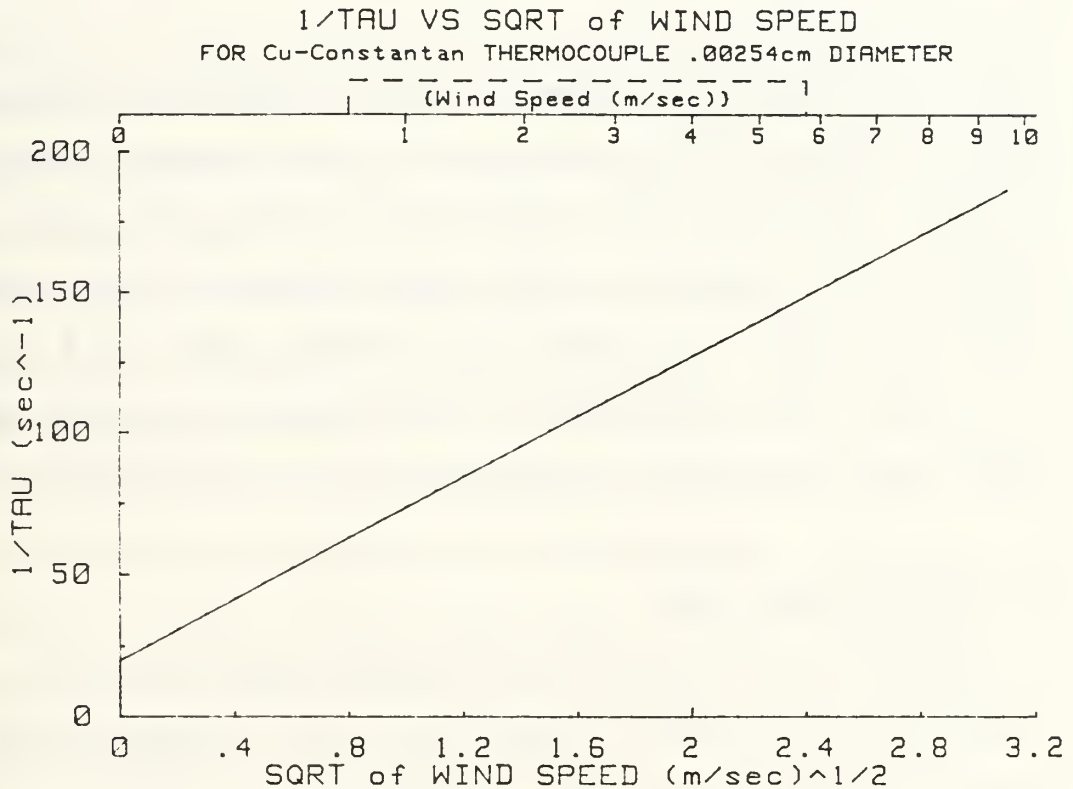


Figure 11. Response Time Versus Wind Speed of a .00254 cm Copper-Constantan Thermocouple.

The reason for the fine wire was to reduce the thermal mass which decreases the response time of the thermocouple to temperature change. The response time is defined as the time required to reach 63.2% of an instantaneous temperature change. The OMEGA Handbook [Ref. 20] gives the response time

for a 0.00254 cm thermocouple as 0.05 sec in still air and 0.004 sec in 18.3 m/sec air. The response time τ can be related to the velocity by the equation,

$$\frac{1}{\tau} = A + B\sqrt{V} \quad , \quad (13)$$

where A and B are constants for the specific thermocouple material size and are determined by the response times given in Ref. 20 (for this case $A=20$ and $B=53.783 \text{ sec}^{-1}$). This results in a response time verses velocity curve shown in Figure 11. From this curve the response time τ @ 5 m/sec is .0071 sec. The interaction of the frequency response and the inner scale size will be discussed in the Results section.

C. COMPUTER AND CODE

The data acquisition and processing portion of the system consists of a Hewlett Packard model 217 computer with a 20 megabyte hard drive and 2 megabytes of memory. It also contains an Infotek BC203 Basic compiler, an Infotek AD200 analog to digital converter, an HP9133 floppy disk drive, a monitor and printer. The computer receives data from the circuit via the analog to digital converter. It reduces the data and displays a C_T^2 verses time (altitude) profile.

The analog to digital converter is the primary component for the data acquisition, however it introduces errors. The

A to D converter has a small DC voltage offset. This offset is small so it does not significantly affect the results until C_T^2 reaches values on the order of 10^{-3} , as is discussed in the results section. Each A to D converter has a different offset so each time a different computer is used the offset must be measured. In addition the noise of the electronic circuit produces a DC offset. To find the total DC offset, the entire system was set up and run in the anechoic chamber to insure no external signals are introduced. The software has a feature for inputting the offset and another to display the voltages directly from the probe. To find the offset, initially set the offset to zero and then after the system has run for about one hour, to settle all the air currents generated by the set-up, read the voltages by pressing the PRINT_RAW key, this displays the actual voltage offset then simply reboot the system and input the offset read from the raw voltages. The DC offset for the system used for the experiment was -5 millivolts.

Appendix A summarizes the features of the software and lists the code for controlling and producing output from the system. It is almost fully automatic. Once it has started running, the only corrections to be made are to update the ambient air temperature any time there is a change of two or three degrees, so the Seebeck coefficient can be recalculated. There is a hard function key for updating the air temperature. A further refinement to the system would be to have the

rawinsonde temperature measurement device automatically update the program with the new air temperature at a given interval to make the system fully automatic.

D. SOLAR HEATING

It is important to understand the effects of thermal radiation on the probes since they will be ascending through the atmosphere both during the day and at night. During the day radiative heating from direct and reflected solar radiation will heat the probes above ambient air temperature while at night the probes will be cooled due to Planck radiation from the probes to space. There are several ways in which the heating or cooling of the probes can introduce errors into a differential measurement device. A hot wire anemometer effect can introduce errors. Another is the difference caused by one probe being in the sun and the other being in the shade or at night where one probe has a direct line of sight to the earth and the other is blocked as by a cloud. In a hot wire anemometer effect the probes are heated above the ambient temperature and then velocity fluctuations across the probes vary the heat transfer rates away from the probes, creating a false temperature difference [Ref. 21]. In the sun-shade effect, as the probe ascends through the atmosphere one end may come into shade either from a cloud or

the balloon shadow. The probe may rotate as it ascends giving one thermocouple a different aspect to the sun than the other, creating the same sun/shade effect to a lesser extent. In either case one thermocouple will receive less direct solar radiation than the other thereby changing the heat flow on one thermocouple but not the other, again introducing a false difference. The same applies at night if one thermocouple is shaded from the earth by a cloud it will not radiate thermal energy at the same rate as the other will.

The net heat flow to or from a body in the atmosphere is described by the heat transfer equation,

$$q_{\text{net}} = q_s + q_a + q_t + q_c + q_k - q_r , \quad (14)$$

where q_s = portion of direct solar radiation absorbed

q_a = portion of the atmospheric radiation absorbed

q_t = portion of terrestrial radiation absorbed

q_r = thermal radiation emitted by the wire

q_k = net conduction to the wire from the atmosphere

q_c = net convection to the wire from the atmosphere

[Ref. 22]. The temperature difference can be determined by first setting q_{net} equal to 0. The equation can then be reduced into the heating and cooling portions by,

$$E_{\text{SD}} + E_{\text{SR}} + E_{\text{LE}} = E_{\text{LW}} + E_{\text{C}} , \quad (15)$$

where E_{SD} = heating due to direct solar radiation

E_{SR} = heating due to solar radiative reflection of
the atmosphere

E_{LE} = heating due to long wave radiation from earth

E_{LW} = cooling due to long wave radiation from wire

E_c = convective cooling

[Ref. 23]. If we further assume the thermocouple to be a horizontally oriented, infinite cylinder with the top half radiating to the sky and the bottom half radiating to the earth's surface, the temperature difference between the ambient air and the thermocouple is given by,

$$\Delta T = \frac{\epsilon_s \left[1 + \frac{\pi \alpha}{2} \right] R_s + \pi \epsilon_L \left[\frac{R_a + R_g}{2} - \sigma T^4 \right]}{h} \quad (16)$$

where h = average convective conductance

ϵ_s = short wave emissivity of the thermocouple

ϵ_L = long wave emissivity of the thermocouple

α = albedo

R_s = short wave incoming radiation

R_g = long wave radiation from the earth's surface

R_a = long wave atmospheric radiation

σ = Stephan-Boltzmann constant

T = air temperature

where h is defined by Kreith [Ref. 22] as,

$$h = \frac{Kk}{D} \left[\frac{VD}{\nu} \right]^n, \quad (17)$$

where D = wire diameter

V = wind speed

k = heat conductivity of the air

ν = kinematic viscosity of the air

K&n = empirically determined dimensionless constants
based on the Reynolds number

[Ref. 24].

The Air Force Geophysics Laboratory [Ref. 23] defines the calculation for delta T in a similar manner based on the same assumptions. However, when comparing the two forms using the same parameters (see Figure 12) there is a considerable difference. Review of both treatments shows the principle difference lies in each definition of the convective conductance h. Campbell [Ref. 24] uses Krieth's form of h (EQN 17) while Brown [Ref. 23] assumes an average value. Another method of determining h is with the Nusselt number, which is a dimensionless number used in describing heat transfer and fluid flows. Kramers [Ref. 25] performed extensive measurements of heat transfer on spheres and cylinders, from this he determined the Nusselt number to be a function of the Reynolds number and the Prandtl number, another dimensionless number where,

$$Re = VD\rho/\mu , \quad \text{and} \quad Pr = c_p\mu/k , \quad (18)$$

where D = diameter of the cylinder

V = velocity of the fluid

ρ = density of the fluid

μ = dynamic viscosity of the fluid

k = thermal conductivity of the fluid

c_p = specific heat of the fluid.

From all the available data he showed that the Nusselt number for a cylinder could be represented by,

$$\begin{aligned} Nu &= 0.91(Pr)^{0.31}(Re)^{0.385} , 0.1 < Re < 50 , \\ &\text{and} \\ Nu &= 0.60(Pr)^{0.31}(Re)^{0.50} , 50 < Re < 10,000. \end{aligned} \quad (19)$$

Based on the Nusselt number the convective conductance is,

$$h = Nu*k/D. \quad (20)$$

Campbell included some experimental results in his paper. When the experimental results are compared with Kreith's and Kramers' treatment of h we can see that Kramers' expression exactly models the actual data (Figure 13). Using Equation 20 for h in Equation 16 corrects the differences seen in Figure 12, therefore the lower curve in Figure 12 is the correct

model for solar radiative heating in the atmosphere, based on the results obtained using the experimental data of Reference 24.

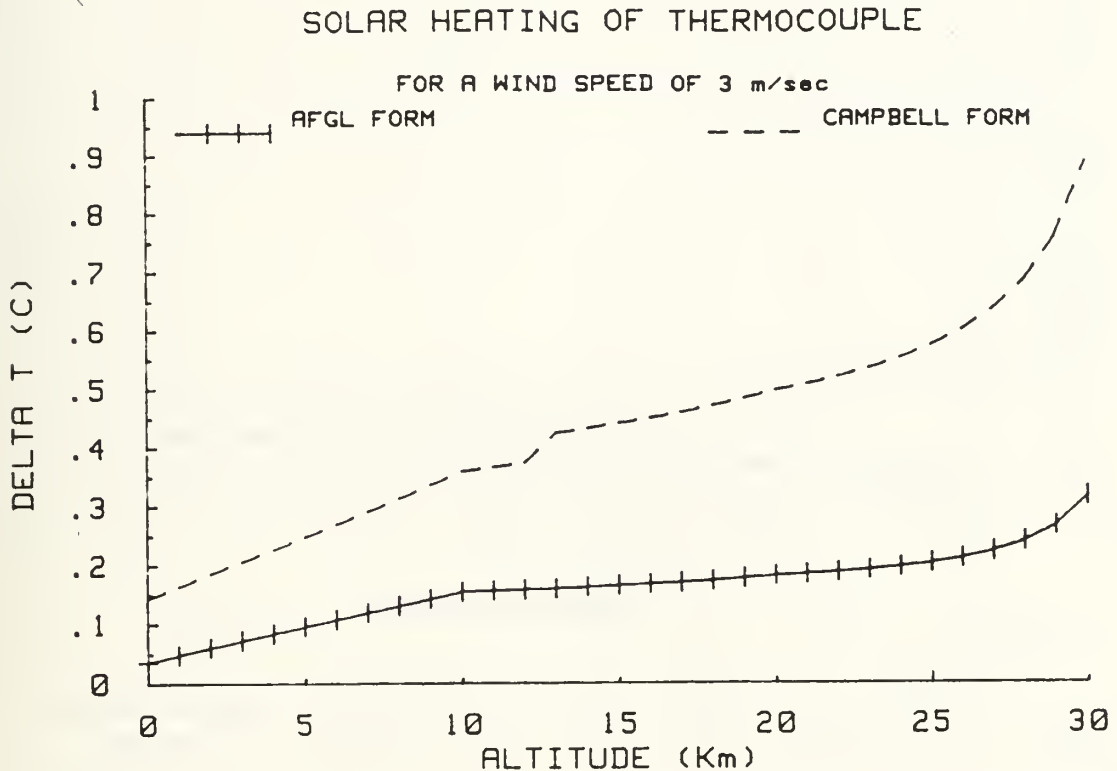


Figure 12. Comparison of AFGL Model and Campbell's Model of Solar Heating of Thermocouple Wires.

A discrepancy noted in Campbell's calculations was the values used for short(visible) and long(IR) wave emissivities. Table 2 gives the emissivities used and the actual emissivities from a 1986 edition of the CRC handbook. The corrected values were used to recalculate the solar heating and the updated results are shown in Figure 14.

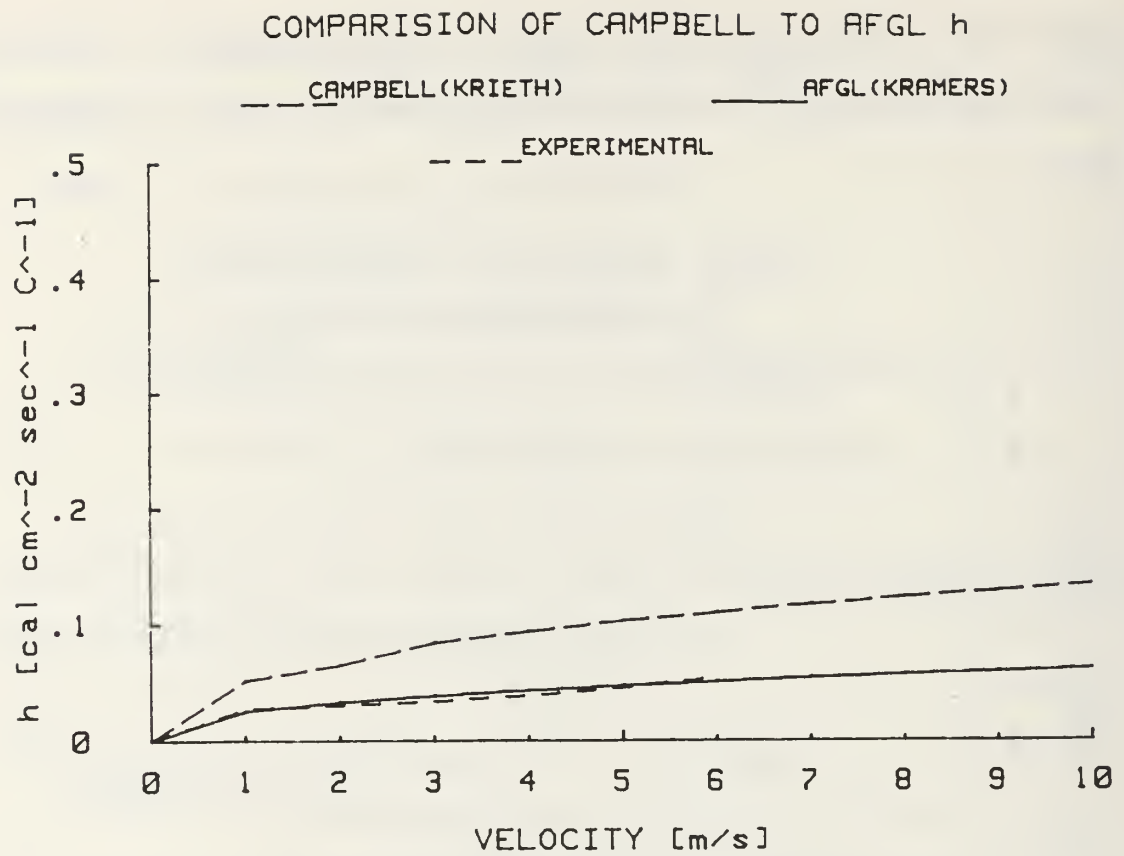


Figure 13. Comparison of Convective Conductance.

Table 2
EMISSIONS OF CU-CONSTANTAN
AND TUNGSTEN

	Visible	IR
Campbell's Cu-Constantan	.25	.5
CRC Handbook Cu-Constantan	.2	.03
CRC Handbook Tungsten	.5	.03

SOLAR HEATING OF THERMOCOUPLE

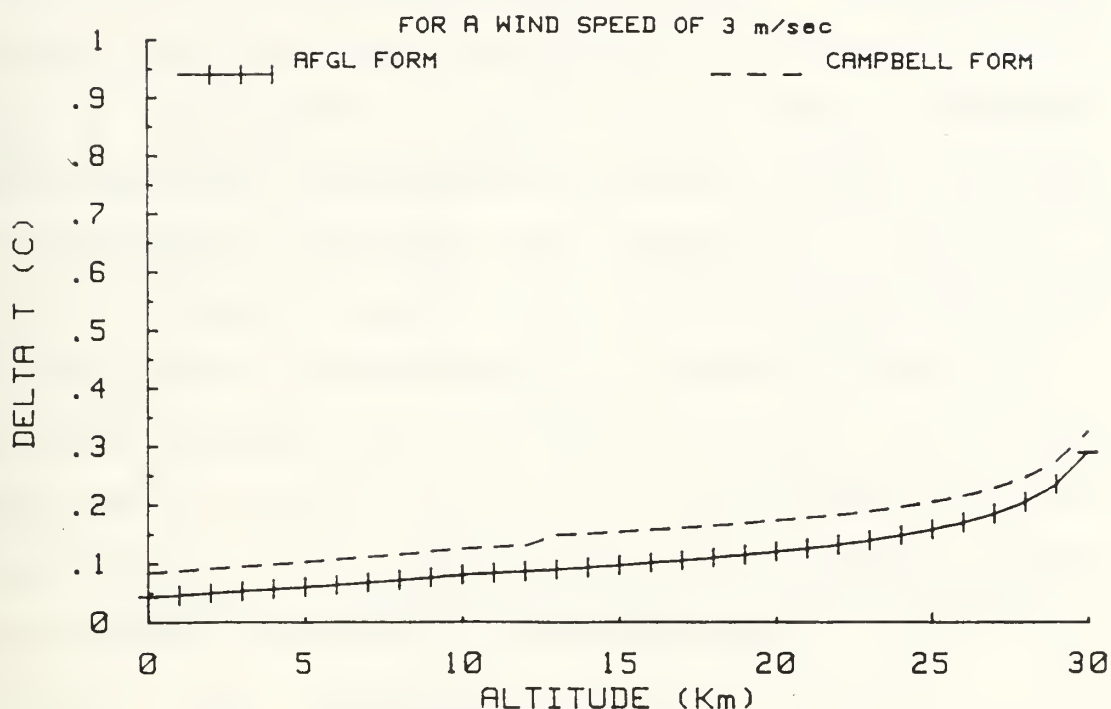


Figure 14. Corrected Comparison of solar heating.

Based on Figure 14 it is now possible to make a determination of the errors introduced by solar heating. The structure function for velocity fluctuations over small scale lengths is,

$$D(r) = 3.83(\epsilon r)^{2/3} , \quad (21)$$

where ϵ is the dissipation rate [Ref. 26]. Actual data shown in Reference 26 from areas of highly turbulent velocity fields indicates the average dissipation rate is on the order of $3 \times 10^{-5} \text{ m}^2 \text{ sec}^{-3}$. For the probe system with r equal to 1 meter

this yields velocity fluctuations on the order of 0.06 m/sec. Figure 15 shows the solar heating errors due to the hot wire anemometer effect with velocity fluctuations of this magnitude. Figure 16 shows the differences between the curves of Figure 15. It indicates the temperature differences are negligible (on the order of .001 degrees or less).

The shading effect can be determined by eliminating the direct solar radiation component in the equation. This will show the maximum error, if it is a matter of the probe changing aspects to the sun the errors will be proportionally less. If direct solar radiation is completely removed there will be very slight heating of the probe, due to incoming terrestrial radiation. The temperature difference between the two probes will be approximately equal to the amount of solar heating on one probe as seen in Figure 14. This indicates a major source of error since the temperature difference at higher altitudes is on the order of 0.2 °C and the balloon can rotate as it ascends.

Based on these calculations if some method is devised to limit the rotation of the probe to eliminate the sun/shade effect, the probe system can measure C_T^2 values accurately up to 30 km altitude without significant errors.

Reference 7 described a C_T^2 thermosonde used by the Air Force Geophysics Laboratory. Data measured by this system indicates an order of magnitude jump in the values of C_N^2

SOLAR HEATING OF THERMOCOUPLE

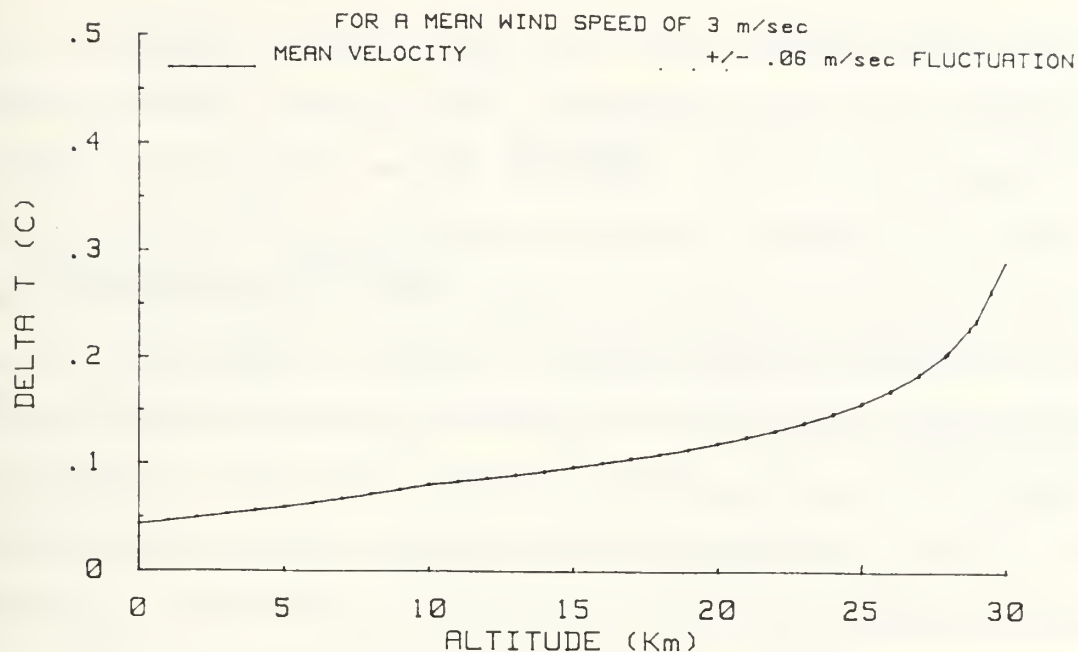


Figure 15. Hot Wire Anemometer Effect on Copper Constantan Thermocouples.

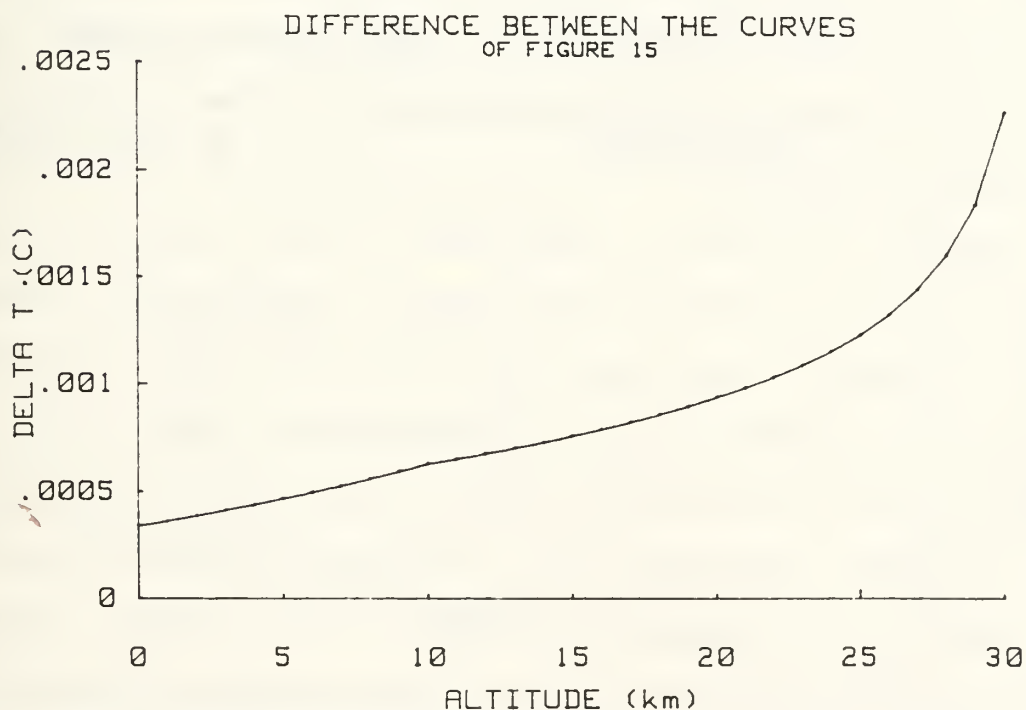


Figure 16. Differences Between the Curves of Figure 15.

just after sunrise [Ref. 27]. This increase appears to be an artifact of the instrument rather than actual turbulent processes due to the fact it occurs so rapidly. Since it occurs at sunrise a logical assumption is that it is due to solar heating, therefore a great deal of time has been spent in determining these effects. Figure 17 shows the hot wire anemometer effect on a 4 micron tungsten resistance wire. The values for the emissivity of Tungsten are taken from Table 2. This indicates solar heating does not effect the measurements of C_T^2 consequently the rise in the value of C_n^2 at sunrise may be actual.

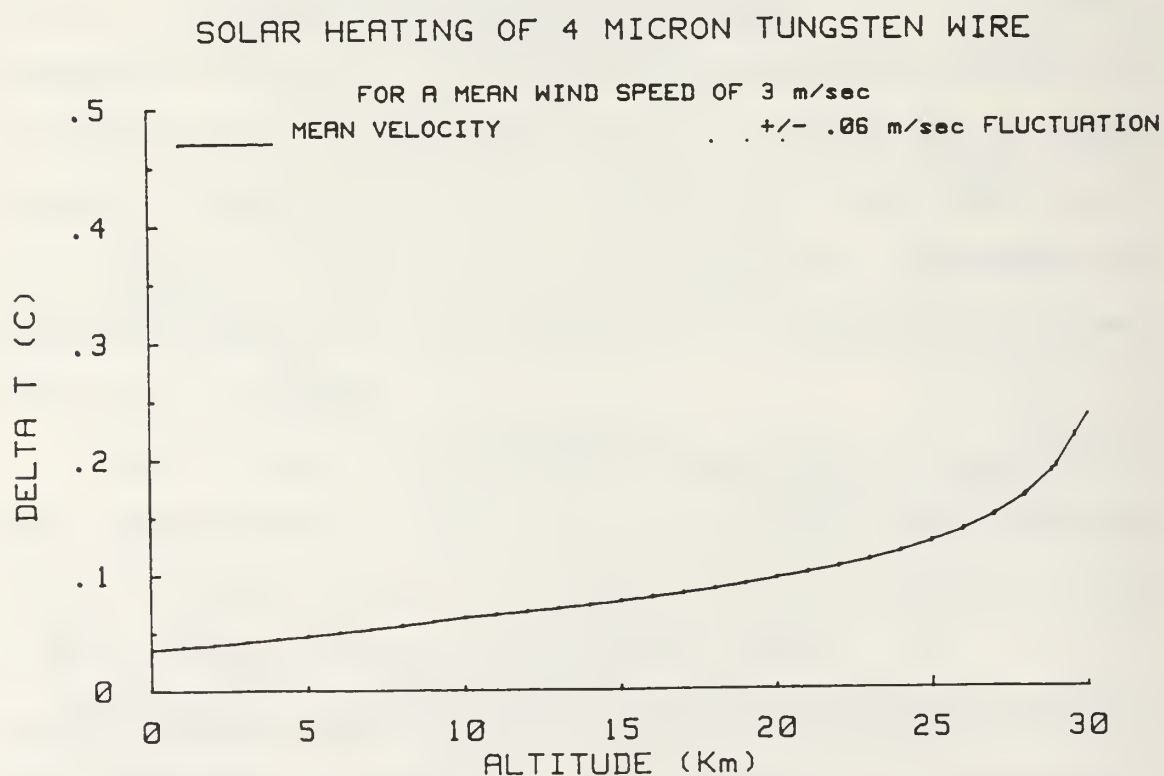


Figure 17. Hot Wire Anemometer Effect on 4 micron Tungsten Wire.

IV. RESULTS

A. EXPERIMENTAL PROCEDURE

The experimental measurements served two purposes, first they were carried out to validate the probe measurement system and second, they were used to validate the C_T^2 measurement capabilities of the acoustic echosounder [Refs. 6,28]. The acoustic echosounder calculates a 15 minute time averaged value for the temperature structure parameter as a function of altitude, however uncertainties in the antenna beam shape, side lobes, transducer efficiencies and atmospheric attenuation produce uncertainties in the absolute value of C_T^2 calculated by the echosounder [Ref. 28]. Therefore independent verification of the C_T^2 values must be made to validate the acoustic echosounder. If both values agree this is a positive indication that both systems are measuring accurately.

The acoustic echosounder is a high frequency device which analyzes the atmospheric density fluctuations within the first 200 meters of the atmosphere. The echosounder consists of a Hewlett Packard HP 217 computer to control the system and acquire and reduce the data, an HP 3314A function generator which produces the pulsed signals, an amplifier and the array of speakers which acts as a transmitter/receiver. The system operates at 5KHz and produces a 100 cycle sinusoidal burst of

18 acoustic watts. The antenna array consists of 19 piezoelectric speakers in a close-packed hexagonal array enclosed in a 55 gallon plastic trash container lined with lead and foam to reduce side lobes as much as possible. The minimum range of the device is approximately six meters based on the recovery or "ring" time of the speakers and the maximum range is about 200 meters based on the frequency used. Figure 18 is a diagram of the acoustic echosounder layout.

A comparison test was run with the probe system and the echosounder between 1300 and 2030 hours local time on 3 September 1988 on the roof of Spanagel Hall on the grounds of the Naval Postgraduate School at Monterey CA. The acoustic echosounder was placed on the sixth level, northwest corner of the roof while the probe was attached to a rigid pole and extended approximately 1.5 meters off the seventh level of the northwest corner of the roof. In this position the probe was approximately 9.2 meters above the echosounder array, thereby being outside of the echosounder blind zone. Due to the building itself and heating exhaust vents on the eastern side of the building it was necessary to monitor the wind direction to insure the prevailing winds were not passing over the building and picking up heat from the exhausts, which would have greatly affected the data. Therefore wind speed and direction as well as temperature and humidity measurements were taken every 15 minutes to update temperature and humidity

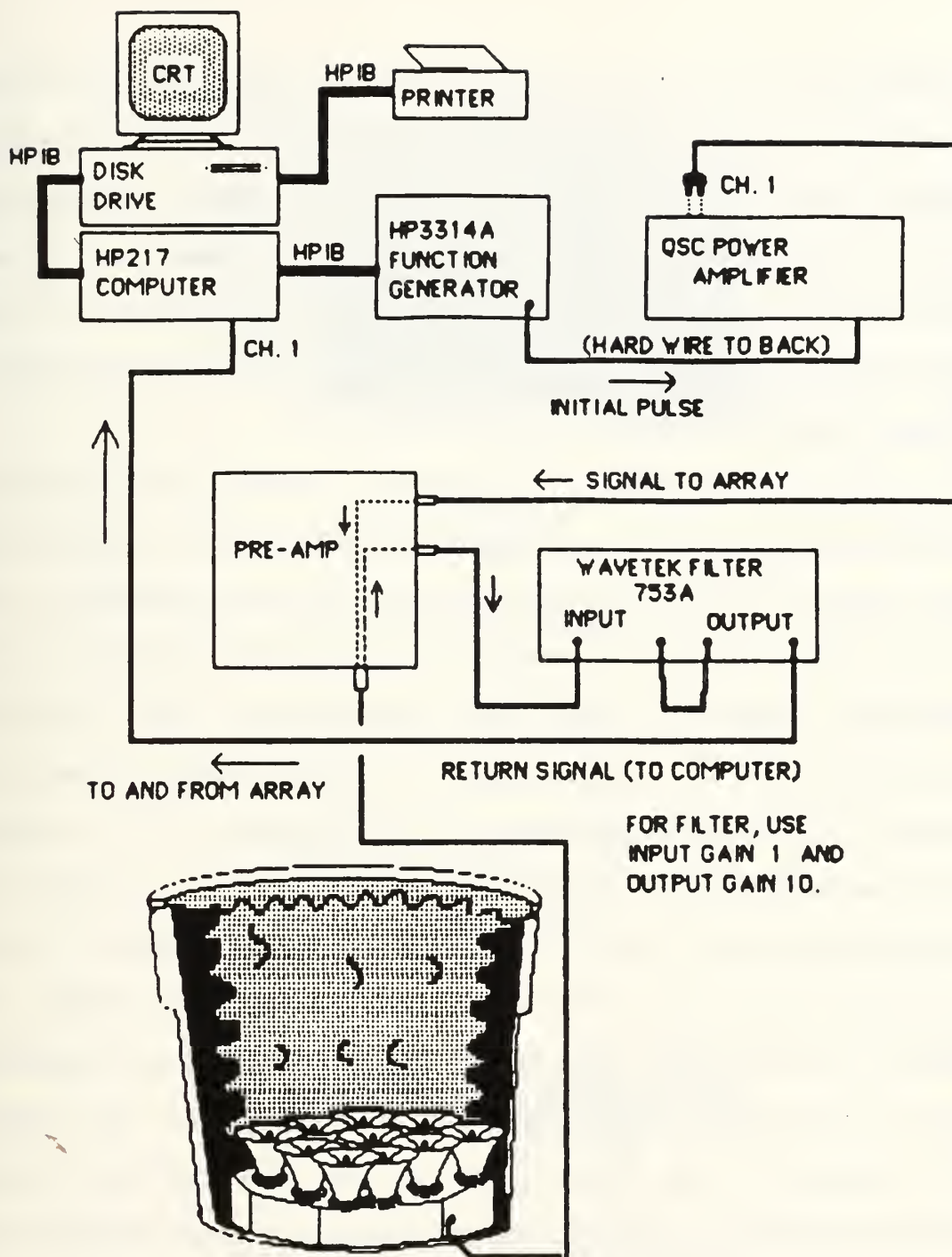


Figure 18. Layout of Acoustic Echosounder Device.[Ref. 28]

information for the two systems as well as determining if the prevailing winds were flowing across the building before passing over the instruments, corrupting the data. During the entire experiment the wind shifted several times but it was always from Northwest to Southwest. At all times the air flow passed over the instruments before passing over the building. All the data was valid.

Figures 19 through 21 represent a portion of the data collected during this experiment. In each of the figures the upper graph is the echosounder profile of the atmosphere, the central graph is a 15 minute time averaged C_T^2 profile of the atmosphere based on the data collected by the acoustic echosounder and the bottom graph is the C_T^2 versus time plot measured by the probe system at an altitude of 9.2 meters above the echosounder. The dark lines below about 6 meters in the upper plot and the discontinuities below 6 meters in the center plot are due to the blind zone of the echosounder. To compare the plots, the average of the bottom plot was compared with the value at an altitude of 9.2 meters in the center plot. Figure 19 was taken early in the afternoon and shows strong convective pluming, which causes a higher temperature structure parameter. Figure 20 which was taken closer to the neutral event shows a marked decrease in the turbulence and a corresponding decrease in the values for C_T^2 . Figure 21

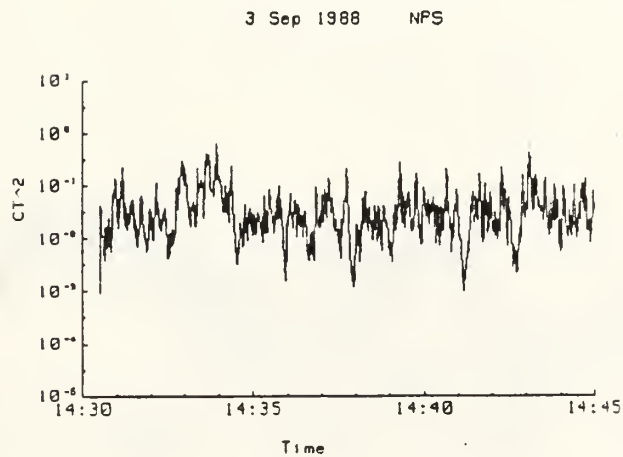
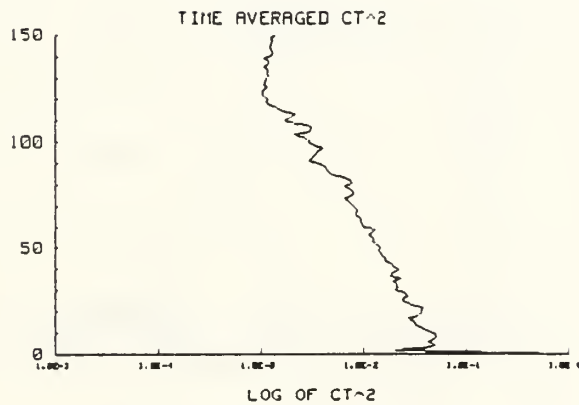
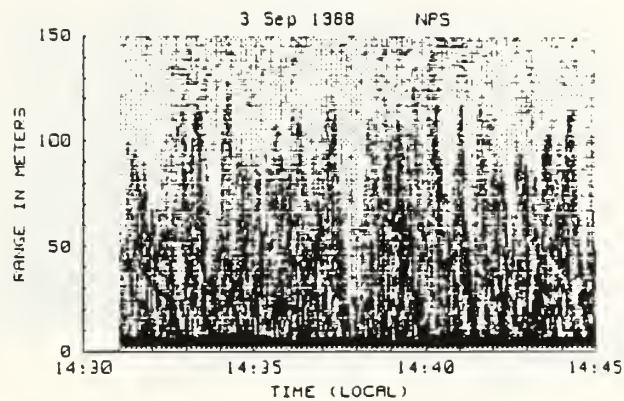


Figure 19. Echosounder Trace and C_T^2 Measurement and Probe Measurement During Strong Turbulence.

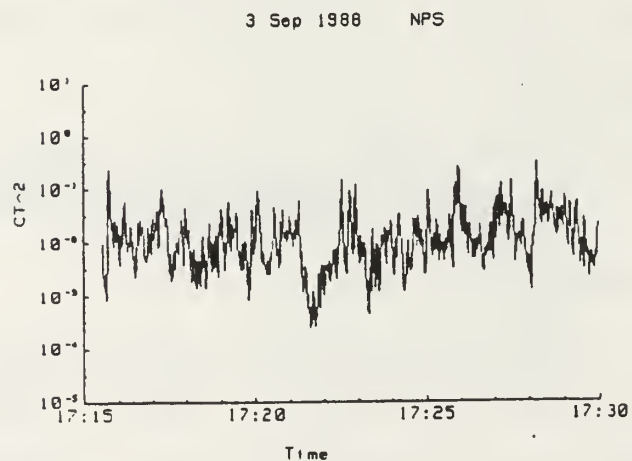
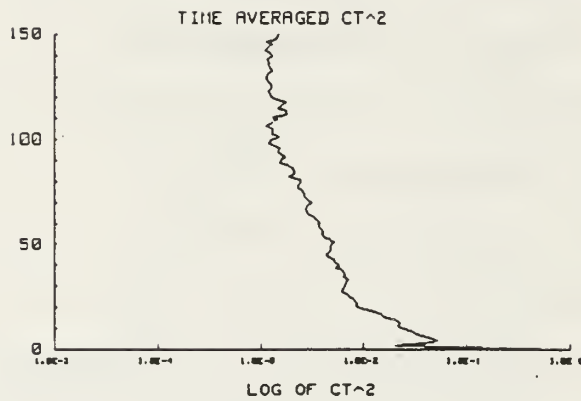
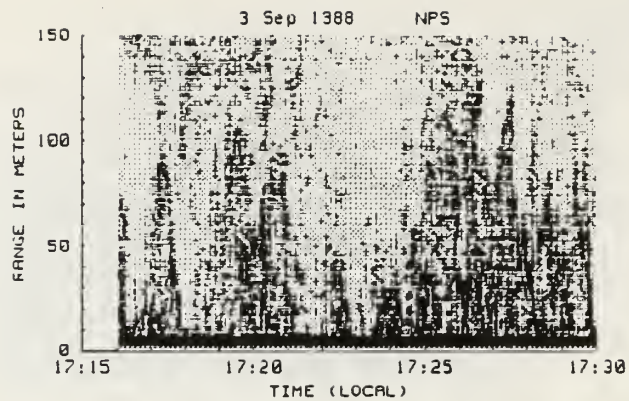


Figure 20. Echosounder Trace and C_T^2 Measurement and Probe Measurement During Light Turbulence.

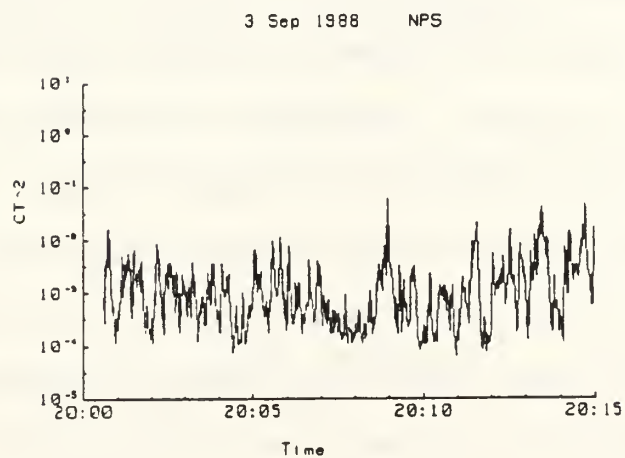
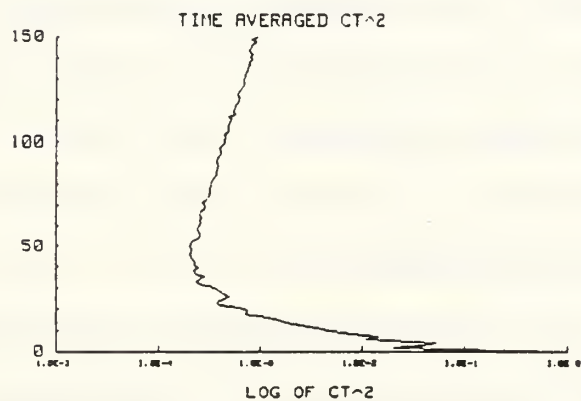
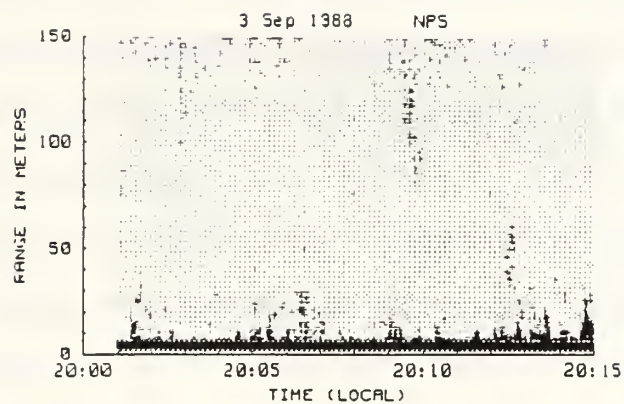


Figure 21. Echosounder Trace and C_T^2 Measurement and Probe Measurement During No Turbulence.

taken during the neutral event, shows virtually no turbulence and a much lower value for C_T^2 . Appendix D contains additional measurements taken during this experiment to show the corresponding increases and decreases in C_T^2 for both the echosounder and the probe system. The purpose of these measurements was not to actually sample the atmospheric processes at this location but to make a quantitative comparison test between the acoustic echosounder and the probe system. For a complete description of the atmospheric turbulence measurements and processes for this location see Weingartner [Ref. 6].

B. SCALE SIZE ERRORS

The temperature variations in a turbulent atmosphere range in size from millimeters to hundreds of meters. Optical aberrations are primarily caused by variations the size of a Fresnel zone $(\lambda D)^{1/2}$ therefore with laser frequencies and path lengths of several kilometers the important scale sizes are on the order of several centimeters.[Ref. 13] With a frequency response of 150 Hz and an average wind speed of 2-5 m/sec, the system is limited to scale sizes greater than 3 cm, which will introduce a small amount of "inner scale" error, since minimum scale sizes are on the order of millimeters, but if used for measurements in conjunction with laser propagation through the

atmosphere the error will be negligible. Additionally, the acoustic echosounder utilizes the smaller scale sizes of approximately 3 cm, thus there will be negligible error introduced by this in a comparison test.

To find the outer scale length errors we can express the structure function of the probe system with limiting scale lengths by,

$$D(a,b) = 4 \int_a^b \frac{(\omega \tau_1)^2}{1 + (\omega \tau_1)^2} \frac{\sin^2(kr/2) k^{-5/3}}{1 + (\omega \tau_2)^2} dk, \quad (22)$$

where a is the limiting lower frequency (outer scale)

b is the limiting upper frequency (inner scale)

$k = 2\pi/\lambda$ where λ is the actual scale length

$\omega = kV$ where V is the wind velocity

$\tau_1 =$ RC time constant of the high pass filter
(the upper frequency cutoff)

$\tau_2 =$ frequency response of the probes
(the lower frequency cutoff)

$r =$ probe separation distance

and comparing it with the structure function over all scale lengths,

$$D(0,\infty) = 4 \int_0^\infty \sin^2 \left[\frac{kr}{2} \right] k^{-5/3} dk, \quad (23)$$

the outer scale length limiting error can be determined. Figure 22 is a graphical representation of this comparison,

showing the error over a range of limiting outer scale lengths. The 8% limiting error on the low end of Figure 22 is due to the high frequency cutoff of the circuit and as the scale size decreases the larger low frequency errors of the circuit begin to dominate, increasing the error. The limiting scale length for the experiment can be determined as the height above ground, which was approximately 30 meters. From Figure 22 it is clear the error introduced due to finite outer scale lengths is approximately 12%. The design of the acoustic echosounder is resistant to outer scale errors therefore the finite inner and outer scale error introduced would cause the probe system to record measurements approximately 12% lower than the echosounder.

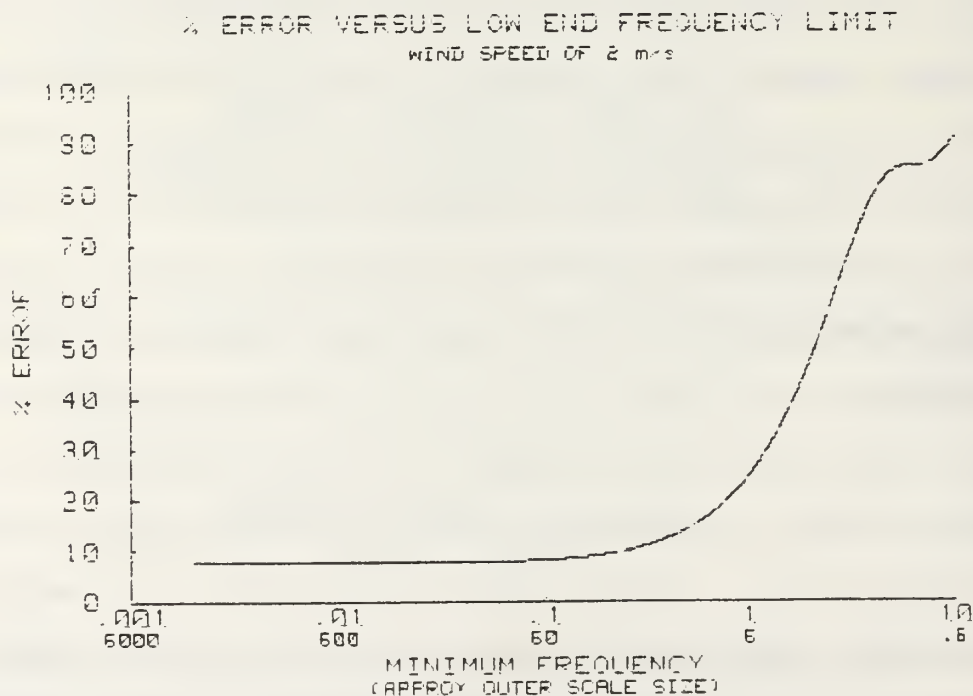


Figure 22. % Error Induced by a Limiting Outer Scale Length

The acoustic echosounder is susceptible to inner scale errors which will cause it to read higher than the probe system. The inner scale length is inversely proportional to the wind speed and can be expressed as,

$$l_0 = 7.4 (\nu^3 / \epsilon)^{1/4}. \quad (24)$$

Ochs and Hill [Ref. 29] made extensive measurements of the inner scale length, based on their results and the mean wind speed of 6 m/sec during the measurements, the approximate inner scale length was 3 mm. At the edge of the inner scale of turbulence there is a bump in the temperature spectrum due to diffusion as it enters the viscous-convective range. Figure 23 illustrates this bump showing the spatial power spectrum Φ_T of temperature fluctuations versus the scaled wave number $\kappa\eta$, which is the wave number normalized by the inner scale length. [Ref. 30] Here κ is equal to $2\pi/\text{Scale Length}$ and η is equal to $l_0/7.14$ (for air). The limiting inner scale size of the echosounder is 3.4 cm ($\lambda/2$ where $\lambda = (340\text{m/sec}) \div (5\text{kHz})$) therefore with an inner scale size of 3mm the scaled wave number is approximately 9×10^{-2} . Figure 23 shows the acoustic echosounder will read approximately 5% higher than the Kolomogorov spectrum and therefore 5% higher than the probe system.

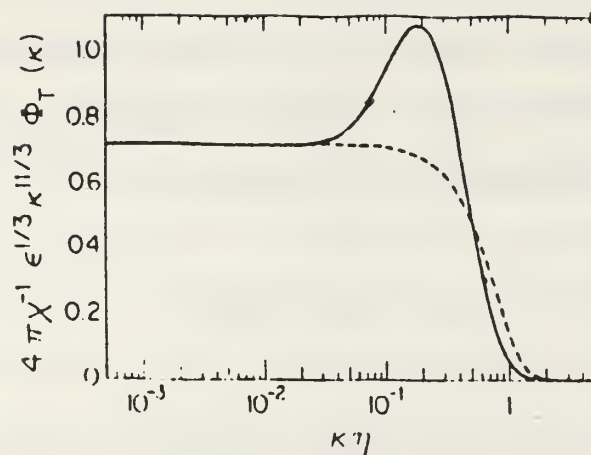


Figure 23. Spatial power spectrum Φ_T of temperature fluctuations versus scaled wave number $\kappa\eta$. Solid curve is actual model; the dashed curve is Tatarski's model. [Ref. 30]

C. ANALYSIS OF DATA

Figure 24 is a comparison of 15 minute time averaged data collected from the echosounder and the probe system. This data was taken before the noise measurements and discovery of the 5 millivolt DC offset error in the A to D converter RMS module combination. Figure 25 shows the corrected data comparing the two systems. The data clearly shows the correlation of the two systems even with the volatile trends of the turbulent fluctuations. It also shows a decrease in the temperature structure parameter leading up to and during the neutral event, which corresponds with the actual physical processes

CT**2 DATA
NPS ROOF 3 SEP 1988

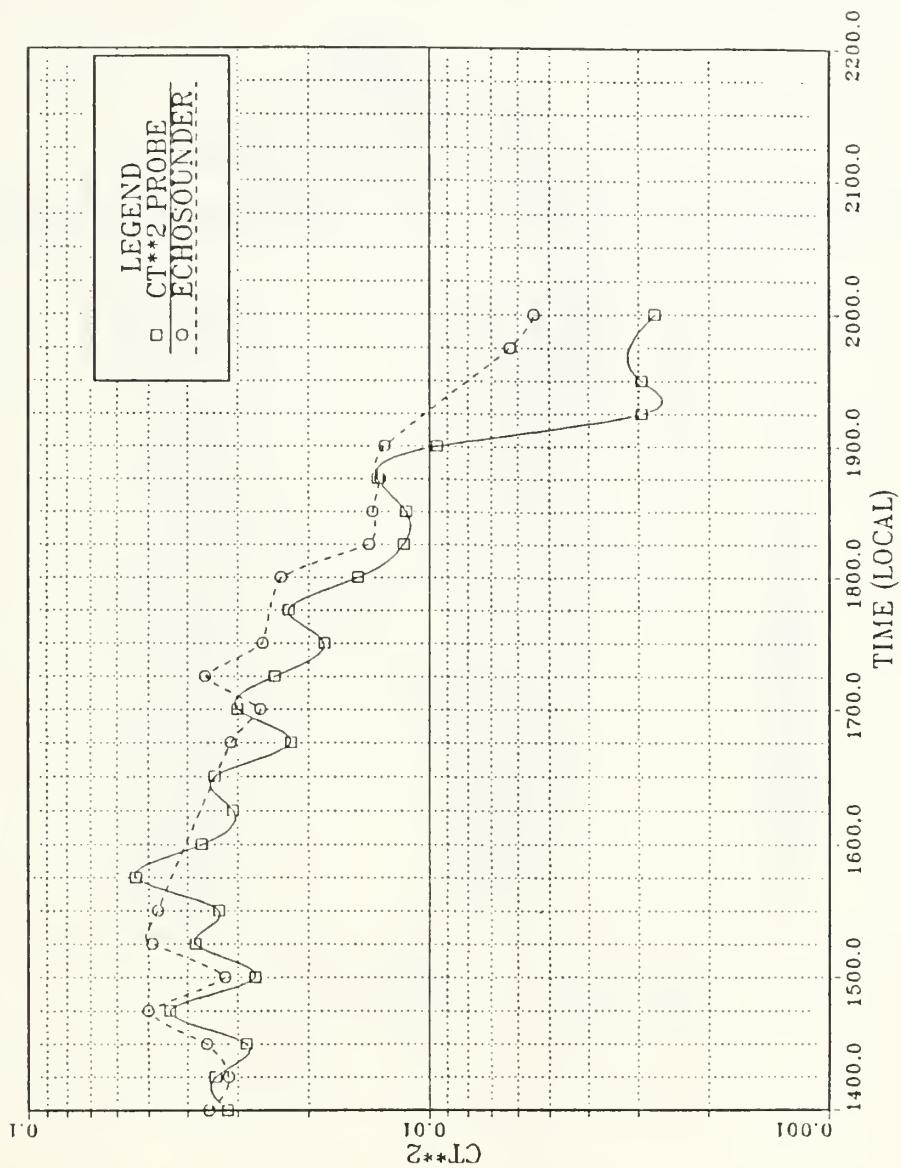


Figure 24. Comparison of Data From Acoustic Echosounder and Temperature Probe Before Correction for DC Offset.

CT**2 DATA
UPDATED WITH DC OFFSET

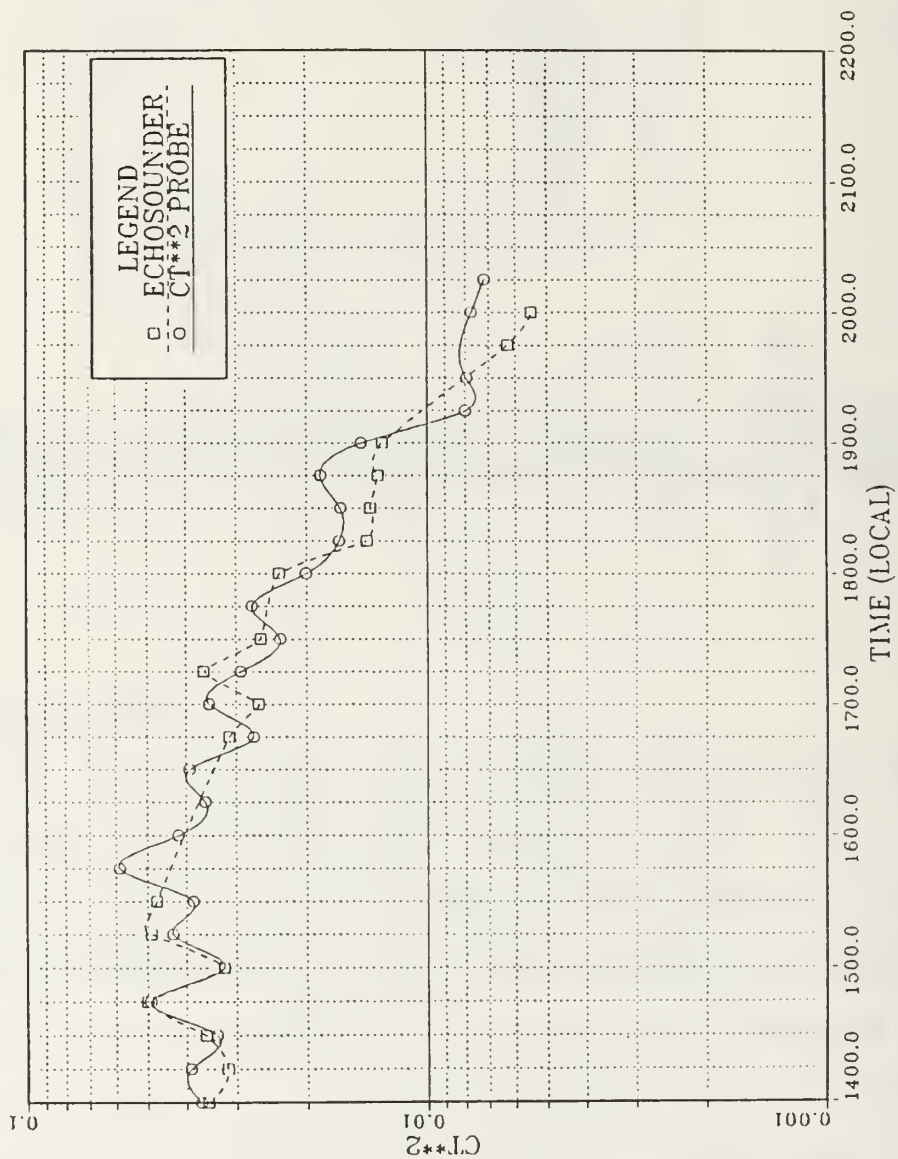


Figure 25. Comparison of Data From Acoustic Echosounder and Temperature Probe After Correction for DC Offset

TABLE 3
 C_T^2 MEASUREMENTS
 (CORRECTED FOR DC OFFSET)

TIME (LOCAL)	ECHOSOUNDER	PROBE	% DIFFERENCE
1400	.0354184	.0368390	3
1415	.0316086	.0391012	23
1430	.0358514	.0335893	6
1445	.0500970	.0492531	2
1500	.0322137	.0321643	0
1515	.0490100	.0432243	12
1530	.0474621	.0384319	20
1645	.0311984	.0271304	13
1700	.0263566	.0350252	32
1715	.0361568	.0292298	20
1730	.0260007	.0232678	10
1745	.0217524	.0274032	25
1800	.0233976	.0200511	14
1815	.0141386	.0165680	17
1830	.0138539	.0165680	18
1845	.0132466	.0184468	39
1900	.0129296	.0145711	15
2000	.0054777	.0077345	40
2015	.0058262	.0071837	23
AVERAGE % DIFFERENCE			17

going on at the time. With the approach of sunset, at 1933 local time, the sun heated the earth's surface to a lesser degree thereby reducing the temperature difference between the earth's surface and the air, which in turn reduced the temperature structure parameter and the turbulence.

Table 3 contains the values of C_r^2 measured by each of the devices and corrected for the offset, it indicates an average difference of 17%, with the probe system reading lower. The scale length errors indicate the probe should read approximately 12% lower due to outer scale length errors and 5% lower due to inner scale bump errors. Therefore there is no significant difference between the probe system readings and the echosounder calculations.

V. CONCLUSIONS

Independent verification of C_T^2 values measured by the acoustic echosounder is important [Ref. 28] and the differential temperature structure parameter probe has provided a valuable comparison indicating the absolute C_T^2 values of both the echosounder and the probe are valid. Taking into account all known errors there is no significant difference between readings of the echosounder and the probe system, which is an extremely good indication that both systems are providing valid measurements. Additionally this thesis demonstrated that solar heating of the probes in the atmosphere does not appear to play as significant a role as first thought. The only major effect solar heating has on the differential system is when one probe is directly illuminated by solar radiation while the other is shaded.

This probe system has many applications including being placed on towers to calibrate other turbulence measuring devices as well as being attached to a rawinsonde system and launched to measure the vertical profile of C_T^2 . When used in this mode it can measure values of C_T^2 up to 30 km altitude accurately, however if it rotates as it ascends through the atmosphere the sun/shade effect of solar heating will

adversely affect the system. Further developments to the package, such as addition of wind vanes on the probe assembly which will not affect the turbulent flow but will dampen the rotation, or a small motor with a flywheel to act as a gyroscopic stabilizer to prevent the probe from rotating, will eliminate the errors induced by this effect.

Other improvements to the system include methods to automatically update the temperature into the program from the balloon systems onboard temperature sensor. Another improvement would be to increase the data transmission rate of the rawinsonde telemetry system to get a higher resolution profile of the thin stratified layers of the turbulent atmosphere or even possibly having the system transmit an AC signal from which a great deal more information can be extracted such as the power spectral density of the turbulence.

APPENDIX A

PROBE SYSTEM SOFTWARE

The program that runs the system is called "CTSQR". It controls the probe system, collects the data, reduces it, and then displays and stores it for further analysis. It is based on the same program that controls the acoustic echosounder. It can be broken down into several sections. The first section sets up the system, initializes all arrays, creates a data file which can store up to eight hours of data and sets up the function keys which are used to update the temperature used in calculating the Seebeck Coefficient, prints out raw voltage data or ends the program storing what has been collected. The next section initializes the Infotek AD200 analog-to-digital converter, which collects the data. Now that the system is ready to collect data it calculates the Seebeck Coefficient based on the information input at start-up or updated through the function key. Next it collects data every second and averages it over ten seconds, reduces it to C_T^2 and plots it every ten seconds. Every 15 minutes it prints out the plot and then resumes the data collection. The program "CTREADER" can take the data file generated by "CTSQR" and read it and calculate 15 minute time averaged values of C_T^2 .

```

10  | RE-STORE "CTSQR2",700,1,0"
20  | CTSQR: 15 SEP 1988: MRD
30  | This program collects one data channel from a HP 3421A or AD converter.
40  | and stores eight hours of the binary data on a disc file
50  |
60  | OPTION BASE 1
70  | Initialize the arrays
80  | DIM Dss(16),Disc_addresses(20),File1$(30)
90  | INTEGER I,J,J4,K,Kstart,Kand,N,Nrec,Hr,D2(2880,4),Plotnum,Print_key
100  |   | D2 = The reduced data output array (2880,4)
110  |   | = (Day,Hr, VDLTS_AVG, CT)
120  |   INPUT "ENTER AIR TEMP (DEGREES C)",T
130  |
140  | Set constants
150  |   Disc_addresses$=":700,0,6" | HP1B address of disc
160  |   Gain=50000 | Amplifier gain
170  |   Maxrec=2880 | # records in output file
180  |   Nplot=900 | # points plotted
190  |   Plotnum=0
200  |   Print_key=1 | print raw data if >0
210  |   R=1.0 | Probe separation (m)
220  |   Scale=10000 | Disc storage scale factor
230  |   | The Equation For The Seebeck Coefficient
240  |   See=3.8707E-2+0.5348E-5*T-3.3135E-7*T^2
250  |   Beck=-2.77432E-9*T^3-1.253E-11*T^4
260  |   Seebeck=(See+Beck)*1.E-3
270  |   PRINT Seebeck
280  |   |
290  |   R_one_third=R*(1./3.)
300  |   |
310  | SET TIME$
320  |   INPUT "DO YOU WANT TO RESET THE CLOCK (Y OR N)?",D$
330  |   IF D$="Y" THEN
340  |     INPUT "ENTER "DD MMM YYYY" (Local Time)",Date$
350  |     INPUT "ENTER "HR:MIN:SC" (Local Time)",Time$
360  |     SET TIME$ DATE(Date$)+TIME(Time$)
370  |     PRINT DATE$(TIME$),TIME$(TIME$)
380  |     Tstart=TIME$
390  |     T0=Tstart MOD 86400
400  |   END IF
410  |   INPUT "INPUT SITE NAME",Site$
420  |   INPUT "ENTER THE A-D CONVERTER OFFSET(-.005 FOR HP 217)",Zero
430  |   INPUT "ENTER THE LOWEST DECADE FOR THE PLOT (NORMAL USE -5)",Ymin
440  |
450  | Create_file:
460  |   | Set up the data reduction output file
470  |   INPUT "ENTER REDUCED DATA OUTPUT FILE NAME",File1$
480  |   File1$=File1$&Disc_addresses$
490  |
500  |   INPUT "1ST ENTRY IN REDUCED OUTPUT FILE? (YES OR NO)",D$
510  |   IF D$="NO" THEN GOTO Didfile
520  |   Newfile: CREATE BDATA File1$,1,23040 | 2 BYTES x FILE SIZE 8 HOURS OF DATA
530  |   ASSIGN #File1 TO File1$
540  |   Nrec=0 | # OF ENTRIES IN THE OUTPUT FILE
550  |   GOTO Setup
560  |   Didfile: ASSIGN #File1 TO File1$
570  |   ENTER #File1:D2(*)
580  |   ASSIGN #File1 TO File1$ | GO TO START OF FILE
590  |   Nrec=D2(1,1) | THE OLD # OF ENTRIES IN THE OUTPUT FILE
600  |   Setup: | Set up the data reduction and plot format
610  |   OUTPUT KBD:"SCRATCH KEY": | Clear keys
620  |   CONTROL 2,2:1 | Select user menu 1
630  |   ON KEY 1 LABEL "PRINT RAW" GOTO Print_raw
640  |   ON KEY 8 LABEL "Quit" GOTO Quit
650  |   ON KEY 2 LABEL "UPDATE TEMP" GOTO Update_temp
660  |
670  |   Npoint=TIME$ MOD 86400 MOD 3600 DIV 15
680  |   CALL Plotsetup(Nplot,Site$,Ymin)
690  |   CALL Init_ed200 | Initialize A-D
700  |   OUTPUT KBD: "L": | Turn on graphics
710  |
720  |   | Begin the main data acquisition loop
730  |
740  |   WHILE Nrec<=Maxrec
750  |     Start_lo: |

```

```

760 Voltsq=0
770 Store_date=0
780 FOR I=1 TO 10
790 Sync: I Synchronize data collection with the system clock
800 T1=INT(TIMEDATE MOD 86400)
810 IF T1<T0 THEN T0=T0-86400
820 IF (T1-T0)<1 THEN GOTO Sync
830 T0=T1
840 Read_ad: I
850 CALL Adin(Voltage,Zero) I Read Infotek A-D
860 IF Print_key>0 THEN
870 PRINT USING "100.0000";Voltage
880 GOTO Read_ad
890 END IF
900 Voltsq=Volsq+Voltage*Voltage I Average voltage^2
910 Npoint=INT(T1 MOD 3600 MOD Nplot)
920 IF Npoint<Npoint_old THEN Store_date=1
930 IF Npoint_old>0 AND Store_date=0 THEN
940 I Plot the data
950 Ctsqr=(Voltage/(Gain*Seebeck*R_one_third))^2
960 Lqtsqr=L6T(Ctsqr)
970 I MOVE Npoint_old,Volts_old
980 I DRAW Npoint,Voltage I Plot Voltage
990 MOVE Npoint_old,Lqtsqr_old
1000 DRAW Npoint,Lqtsqr
1010 END IF
1020 Volts_old=Voltage
1030 Lqtsqr_old=Lqtsqr
1040 Npoint_old=Npoint
1050 IF Store_date=1 THEN Npoint_old=0
1060 NEXT I
1070 Volts_avg=SQR(Volsq/10)
1080 Ct=Volts_avg/(Gain*Seebeck*R_one_third)
1090 DISP " "
1100 T1=TIMEDATE
1110 Day%=DATE$(T1)
1120 Time%=TIME$(T1)
1130 I
1140 I *** CT SQUARED DATA REDUCTION SECTION ***
1150 I
1160 Yr%=Day%12,11)
1170 Day=((DATE$(Day%)-DATE$("1 JAN "&Yr%)) DIV 86400)+1
1180 I
1190 Nrec=Nrec+1
1200 I CALCULATE DECIMAL HOURS
1210 Ts=Time%
1220 Hours=VAL(Ts(1,2))+VAL(Ts(4,5))+VAL(Ts(7,8))/60/60
1230 Hr=1000*Hours I Note that the HP rounds
1240 PRINT "Record ";Nrec:" Collected ";Day%:" ";Time%
1250 PRINT " "
1260 ALPHA OFF
1270 I SET UP OUTPUT ARRAY
1280 N1=Nrec+1 IFOR OPTION BASE 1
1290 D2(1,1)=Nrec
1300 D2(1,1)=Day
1310 D2(1,2)=Hr
1320 D2(1,3)=Volts_avg*Scale
1330 D2(1,4)=Ct*Scale I Intensity
1340 PRINT N1:D2(1,1):D2(1,2):D2(1,3):D2(1,4)
1350 Store_date: I Write output every NPLDT seconds
1360 IF Store_date=1 THEN
1370 Store_date=0
1380 PRINT
1390 DISP "WRITING REDUCED OUTPUT"
1400 OUTPUT #File1:D2(*)
1410 ASSIGN #File1 TO File1$
1420 Plctnum=Plctnum+1
1430 IF Plctnum MOD 2=1 THEN
1440 PRINTER IS 701
1450 PRINT "

```

```

1460          PRINTER IS 1
1470      END IF
1480      DUMP GRAPHICS $701      ! Dump screen to printer
1490      Nprint=0
1500      DISP " "
1510      CALL Plotsetup(Nplot,Sites)
1520      END IF
1530 End_whilea: END WHILE
1540 !
1550 Update_temp: ! Updates Seebach Coefficient With New Air Temp
1560      INPUT "ENTER NEW AIR TEMPERATURE(DEGREES C)",T
1570      See=3.8707E-2+8.5340E-5*T-3.3135E-7*T^2
1580      Beck=-2.77432E-9*T^3-1.253E-11*T^4
1590      Seebach=(See+Beck)*1.E-3
1600      GOTO Start_lo
1610 Print_raw: ! TOGGLE THE PRINT FLAG
1620      Print_key=-Print_key
1630      GOTO Start_lo
1640 Quit: ! Write reduced data output file
1650      FOR I=1 TO N1
1660          PRINT I:D2(I,1):D2(I,2):D2(I,3):D2(I,4):D2(I,5):D2(I,6)
1670      NEXT I
1680      OUTPUT #FileI:D2(*)
1690      PRINT "DATA FILE HAS BEEN STORED UNDER NAME",FileI$
1700      BEEP
1710      BEEP
1720      ASSIGN #FileI TO *
1730      STOP
1740      END
1750      SUB Plotsetup(Nplot,Sites,Ymin)
1760          Ymax=1
1770          GINIT
1780          GRAPHICS ON
1790          LINE TYPE 1
1800          VIEWPORT 15,120,15,00
1810          WINDOW 0,Nplot,Ymin,Ymax
1820          AXES 60,.5,0,Ymin,5,2
1830          CLIP OFF
1840          CSIZE 4,.6
1850          LOPG 6
1860 ! Draw Log Y Axis
1870 ! FOR Decade=Ymin TO Ymax
1880 !     FOR Units=1 TO 1+8*(Decade<Ymax)
1890 !         Y=Decade+LGT(Units)
1900 !         MOVE 0,Y
1910 !         DRAW Nplot,Y
1920 !     NEXT Units
1930 ! NEXT Decade
1940 ! Label horizontal axis
1950      T1=TIMEDATE MOD 86400
1960      Hrs=T1 DIV 3600
1970      T2=T1 MOD 3600
1980      Min=T2 DIV 60
1990      Qtrhr=Min DIV 15
2000      FOR M=0 TO Nplot STEP 300
2010          MOVE M,Ymin-.06
2020          Qtrmin=Qtrhr+15+(M/300)*5
2030          IF Qtrmin=60 THEN
2040              Qtrmin=0
2050              Hrs=Hrs+1
2060          END IF
2070          LABEL USING "DD,A,ZZ":Hrs:"":Qtrmin
2080      NEXT M
2090      MOVE Nplot/2,Ymin-.8
2100      LABEL "Time (Local)"
2110 ! Label Ordinate
2120      LOPG 8
2130      FOR M=Ymin TO Ymax
2140          LOPG 8
2150          CSIZE 4
2160          MOVE -Nplot/23.3,M
2170          LABEL USING "#,K": "10"
2180          CSIZE 2
2190          LOPG 1
2200          MOVE -Nplot/20,M
2210          LABEL USING "#,K":M
2220      NEXT M

```



```

2090      NEXT M
2090      MOVE Nplot/2,Ymin-.0
2100      LABEL "Time (Local)"
2110      Label Ordinate
2120      LORG 0
2130      FOR M=Ymin TO Ymax
2140          LORG 0
2150          CSIZE 4
2160          MOVE -Nplot/23.3,M
2170          LABEL USING "%,K";"10"
2180          CSIZE 2
2190          LORG 1
2200          MOVE -Nplot/20,M
2210          LABEL USING "%,K";M
2220      NEXT M
2230      LOIR P1/2
2240      LORG 5
2250      CSIZE 4
2260      MOVE -Nplot/7,(Ymin+Ymax)/2
2270      LABEL "LOG OF CT^2"
2280      Title the plot
2290      LOIR 0
2300      LORG 4
2310      MOVE Nplot/2,Ymax+1
2320      LABEL DATE$(TIMEDATE);"      ":Site$
2330      CLIP ON
2340      SUBEND
2350      SUB Adin(Voltage,Zero)
2360          ! 26 APR 1985: OLV
2370          ! INFOTEK A-D Input routine set up for internal trigger
2380          ! and average 40 points over three 50 Hz cycles
2390          !
2400          INTEGER I,Npoints,Ad_data(1:40)
2410          DIM Select$(20)
2420          Ad_sel_code=17
2430          Intensity=0
2440          Npoints=40
2450          Counts=VAL$(Npoints)
2460          Scale=5.0/(Npoints*2047.)
2470          Stdev=0
2480          Delta_time$="1250000"      ! AD interval between samples in naac
2490          Select$="select 1sl end"
2500          GOSUB Read_ad
2510          FOR I=1 TO Npoints
2520              Voltage=Voltage+Ad_data(I)
2530          NEXT I
2540          Voltage=(Voltage-Zero)*Scale
2550          GOTO Subend
2560      Read_ad:      ! Read the Infotek A-D
2570          ! Initialize the A-D
2580          OUTPUT Ad_sel_code:"RESET","internal","count",Counts
2590          OUTPUT Ad_sel_code:"time",Delta_time$,"delayon",Select$
2600          OUTPUT Ad_sel_code:"STATUS"
2610          ENTER Ad_sel_code:Resp$
2620          IF Resp$="-----" THEN
2630              ENTER Ad_sel_code USING "%,W";Ad_data(*)
2640              OUTPUT Ad_sel_code:"STATUS"
2650              ENTER Ad_sel_code:Resp$
2660              IF Resp$<>"-----" THEN
2670                  PRINT "ERROR DURING SAMPLING = ":Resp$
2680              END IF
2690          ELSE
2700              PRINT "ERROR DURING A-D INITIALIZATION = ":Resp$
2710          END IF
2720          RETURN

```

```
2730 Subend: 1
2740 SUBEND
2750 SUB Init_ad200
2760 INITIALIZE AD_200
2770 Code=17
2780 Dummy=READIO(Code,3)
2790 WRITEIO Code,0:0
2800 CONTROL Code,0:1
2810 SUBEND
```

APPENDIX B

SOLAR HEATING PROGRAM

```

10 RE-STORE "ALTPLOT",700,1,3"
20 13 OCT 1999 MRC
30 THIS PROGRAM PLOTS THE CHANGE IN THE DELTA T (TEMPERATURE DIFFERENCE
40 BETWEEN THE THERMOCOUPLE AND THE AIR TEMP DUE TO SOLAR HEATING)
50 WITH INCREASE IN ALTITUDE BASED ON GOOD'S CALCULATIONS IN AFGL PUB
60 DATED 23 FEB 1994 AND CAMPBELL'S WORK FROM OCT 1959
70
80 THE FOLLOWING IS THE LIST OF VARIABLES
90
100 J=4.19      mechanical equivalent of heat (W Cal-1 Sec)
110 S=.14       Solar Constant (W cm-2)
120 Epat=.25    Visible Wavelength ABSORPTIVITY of the THERMOCOUPLE
130 Epat=.25    Short Wave Emissivity for CAMPBELL'S Calculations
140 Fd=PI       Form Factor for Direct Radiation
150 Fr=2.       Form Factor for Reflected Radiation
160 Eplw=.5     Long Wave EMISSIVITY of the THERMOCOUPLE
170 Eplw=.5     Long Wave Emissivity for CAMPBELL'S Calculations
180 Ra=.022     Short Wave Incoming Radiation (Cal cm-2 sec-1)
190 Ra=.009     Long Wave Atmospheric Radiation (Cal cm-2 sec-1)
200 Rg=.015     Long Wave Radiation from Ground (Cal cm-2 sec-1)
210 Albedo=.35  Reflection of the Earth
220 Sigma=5.67E-12 Stefan-Boltzmann Constant (W cm-2 K-4)
230 Sigal=1.35509E-12 Stefan-Boltzmann Constant (Cal cm-2 K-4)
240 Dm=.0000254 Probe Diameter in meters
250 Dcm=.00254  Probe Diameter in centimeters
260 Convert=4.189802E+2 Conversion Factor for Thermal Conductivity
270 Beta=1.459E-5 Constant for Determining Mu (kg-1 m-1 K-1/2)
280 Suth=110.4  Sutherland's Constant for Mu (K)
290 Pr=.714     Dimensionless Prandtl Number for Air
300 Re =       Dimensionless Reynolds Number for air
310 Nu =       Dimensionless Nusselt Number for Air
320 T =       Air Temperature (Kelvins)
330 Rho =     Air Density as Function of Altitude (kg/m3)
340 Mu =     Dynamic Viscosity of Air (N-sec/m2)
350 nu =     Kinematic Viscosity of Air (m2/sec)
360 K =     Thermal Conductivity (Cal sec-1 cm-2 (C/cm)-1)
370 h =     Convective Heat Transfer Coefficient ((/ALT))
380         (Cal cm-2 sec-1 K-1)
390 F =     Percentage of Solar Radiation Reaching Given Altitude
400 Qse =    Heat Flux from Earth at Given Altitude (W cm-2)
410 Alt =    The Given Altitude (Km)
420 V =     Wind Speed (m/sec)
430 Kr =     Empirical constant based on Reynolds Number from Krieth
440 In =     Empirical constant based on Reynolds Number from Krieth
450 Delt =   Temperature Difference between TC and Air for GOOD
460 Delt1 =  Temperature Difference between TC and Air for CAMPBELL
470
480
490 INPUT "WHAT WIND SPEED DO YOU WANT",V
500
510 PLOT SETUP
511 INPUT "INPUT 1 FOR PLOTTER OR 2 FOR CRT",Q
512 IF Q=1 THEN PLOTTER IS 707,"HPGL"
513 BE SURE PLOTTER DIP SWITCHES ARE PROPERLY SET 1s. SWITCH 1,2,3 IN POSIT 1
514 IF Q=2 THEN PLOTTER IS CRT,"INTERNAL"
520 SINIT
530 GRAPHICS ON
540 LINE TYPE 1
550 VIEWPORT 15,120,15,80

```

```

550 WINDOW 0,30,0,1
570 AXES 5,.05,0,0,5,2
590 CLIP OFF
590 CSIZE 4,.5
600 LORG 5
610 ! LABEL HORIZONTAL AXIS
620 FOR M=0 TO 30 STEP 5
630     MOVE M,-.04
640     LABEL M
650 NEXT M
660 MOVE 15,-.1
670 LABEL "ALTITUDE (Km)"
690 ! LABEL VERTICAL AXIS
690 LORG 9
700 FOR M=0 TO 1 STEP .1
710     MOVE -.5,M
720     LABEL M
730 NEXT M
740 LOIR PI/2
750 LORG 5
750 MOVE -4.5,.5
770 LABEL "DELTA T (C)"
790 ! TITLE PLOT
790 LOIR 0
900 LORG 4
910 MOVE 15,1.1
920 LABEL "SOLAR HEATING OF THERMOCOUPLE"
930 MOVE 15,1
940 CSIZE 3
950 LABEL "FOR A WIND SPEED OF":U:"m/sec"
950 CSIZE 4
970 !
990 ! Calculations
990 !
990 Altold=0
910 Deltold=0
920 Deltold=0
930 FOR Alt=0 TO 30
940     ! I am assuming the relationship for F and Se are linear wrt Altitude
950     ! The Values were taken from BROWN and GOOD
950     F=.5*(Alt+.012923)
970     Se=.055*(Alt+.00141935)
990     ! The relationships for T,Rho,Mu,Mu, and K are taken from the
990     ! HANDBOOK of GEOPHYSICS and the SPACE ENVIRONMENT chap 14
1000     ! and based on a U.S. Standard Atmosphere
1010     ! This is taken from the Standard Atmosphere Temperature Profile
1020     IF Alt<=10. THEN
1030         T=289.15-7.015*Alt
1040     END IF
1050     IF Alt>10. AND Alt<20 THEN
1060         T=219.
1070     END IF
1080     IF Alt>=20. THEN
1090         T=219.+1.2*(Alt-20.)
1100     END IF
1110     Rho=1.2252-.0399*Alt ! Density Change is approximately Linear wrt
1120     ! Altitude up to about 100 Km
1130     Mu=(Beta*T*1.5)/(T+5uth)
1140     Mu=(Mu/Rho)*.1224255 ! Conversion factor to get correct viscosity
1150     Power=12./T
1160     K1=2.55019E-3*T*1.5
1170     K2=T*245.4*10^Power
1180     K=(K1/K2)/Convert
1190     ! The determination of H was based on KRAMERS (1945) which was shown
1200     ! to more closely approximate experimental results by the plot HPLOT2
1210     Re=Rho*U*On/Mu

```

```

1200 IF Re<50 THEN
1210 Nud=.91*Pr.31*Re-.395
1220 ELSE
1230 Nud=.6*Pr.31*Re-.5
1240 END IF
1250 H=Nud*K/Den
1260 ! Calculations based on BROWN and GOOD (AFGL Pub 1994)
1270 !
1280 ! PRINT "ALT":Alt,"ROW":Row,"MU":Mu,"NU":Nu
1290 ! PRINT " K":K,"Re":Re,"H":H,"T":T
1300 ! PRINT "KRIETH'S H=":Cl,"FIRSTPART=":A1,"2ND=":B1
1310 A=1./(J+H)
1320 B=F+S*Epat*((1./Fd)+(Albedo/Fr))
1330 C=Epatw*((Se/Fr)-(Sigma*T^4))
1340 Delt=A*(B+C)
1350 LINE TYPE 9
1360 MOVE Altold,Deltold
1370 DRAW Alt,Delt
1380 ! Calculations based on CAMPBELL (1959)
1390 !
1400 IF Re<4 THEN
1410 Kr=.991
1420 N=.330
1430 END IF
1440 IF Re<40 AND Re>=4 THEN
1450 Kr=.921
1460 N=.395
1470 END IF
1480 IF Re>=40 THEN
1490 Kr=.615
1500 N=.465
1510 END IF
1520 A1=Epat*Re*(1+((PI*Albedo)/2))
1530 B1=PI*Epat*((Re+Rg)/2)-(Sigma*T^4)
1540 C1=(Den/(Kr*K))*(Nu/(U*Dm))^N ! Krieth's empirical form of 1/h
1550 Delt1=(A1+B1)*C1
1560 LINE TYPE 4
1570 MOVE Altold,Deltold
1580 DRAW Alt,Delt1
1590 Altold=Alt
1600 Deltold=Delt1
1610 Deltold=Delt
1620 PRINTER IS 701
1630 PRINT "ALT=":Alt,"DELT(AFGL)=":Delt,"DELT(CAMPBELL)=":Delt1
1640 NEXT Alt
1650 CSIZE 3
1660 LINE TYPE 9
1670 MOVE 1,.94
1680 DRAW 2,.94
1690 DRAW 3,.94
1700 DRAW 4,.94
1710 MOVE 7,.94
1720 LINE TYPE 1
1730 LABEL "AFGL FORM"
1740 LINE TYPE 4
1750 MOVE 19,.94
1760 DRAW 21,.94
1770 LINE TYPE 1
1780 MOVE 25,.94
1790 LABEL "CAMPBELL FORM"
1800 DUMP GRAPHICS $701
1810 END

```

APPENDIX C

CONDUCTANCE PROGRAM

```

10      RE-STORE "HPLOT2",700,1,0"
20      ! THIS PROGRAM COMPARES THE RESULTS OF THE COMPUTATION OF THE CONVECTIVE
30      ! CONDUCTANCE BY G. CAMPBELL'S METHOD AND BY THE AFGL PAPER'S METHOD
40      ! AND PLOTS THEM AGAINST EXPERIMENTAL VALUES FROM CAMPBELL
50      ! 12 OCT 1989
60      ! VALUES ARE FOR A STD ATMOSPHERE i.e. 1 ATM AT 20 DEG C
70      !
80      Row=1.29      ! kg/m^3 AIR DENSITY
90      Mu=1.71E-5    ! (N-sec)/m^2 DYNAMIC VISCOSITY OF AIR
100     Nu=1.789E-5   ! m^2/s KINEMATIC VISCOSITY OF AIR
110     K=6.175E-5    ! THERMAL CONDUCTIVITY OF AIR
120     D=2.54E-3     ! m DIAMETER OF THE PROBE
130     Pr=.714       ! DIMENSIONLESS PRANDTL NUMBER OF AIR AT 20 DEG C
140     ! KK AND N ARE EMPIRICAL NUMBERS BASED ON THE REYNOLDS NUMBER
150     ! AS DESCRIBED IN KRIETH 1965 pg 411
160     ! U IS THE WIND SPEED IN m/s
170     ! Re IS THE DIMENSIONLESS REYNOLDS NUMBER
180     ! Nud IS THE DIMENSIONLESS NUSSELT NUMBER AS DESCRIBED IN KRAMERS 1946
190     Correct=.7824139225 ! CORRECTION FOR THE EMPIRICAL CALC BETWEEN KRAMERS
200     !
210     ! PLOT SETUP
211     INPUT "INPUT 1 FOR PLOTTER OR 2 FOR CRT",Q
212     IF Q=1 THEN PLOTTER IS 707,"HPGL"
214     IF Q=2 THEN PLOTTER IS CRT,"INTERNAL"
215     ! BE SURE PLOTTER DIP SWITCHES ARE PROPERLY SET i.e. SWITCH 1,2,3 IN POSIT 1
220     ! GINIT
230     ! GRAPHICS ON
240     LINE TYPE 1
250     VIEWPORT 15,120,15,90
260     WINDOW 0,10,0,.5
270     AXES 1,.1,0,0,5
280     CLIP OFF
290     CSIZE 4,.5
300     LORG S
310     ! LABEL HORIZONTAL AXIS
320     FOR M=0 TO 10
330         MOVE M,-.02
340         LABEL M
350     NEXT M
360     MOVE 5,-.07
370     LABEL "VELOCITY [m/s]"
380     ! LABEL VERTICAL AXIS
390     LORG B
400     FOR M=0 TO .5 STEP .1
410         MOVE -.4,M
420         LABEL M
430     NEXT M
440     LOIR PI/2
450     LORG S
460     MOVE -1.5,.25
470     LABEL "h [cal cm^-2 sec^-1 C^-1]"
480     ! TITLE PLOT
490     LOIR 0
500     LORG 4

```



```

510  MOVE S,.6
520  LABEL "COMPARISION OF CAMPBELL TO AFGL H"
530  MOVE S,.4
540  OSIZE 3
550  LABEL "WITH CORRECTION"
560  OSIZE 4
570  !
580  Hold=0
590  Vold=0
600  MOVE 0,0
610  LINE TYPE 5
640  FOR V=1 TO 10
650      Re=Row*V*(D/100.)/Mu
660      IF Re>40000 THEN
670          Kk=.0239
680          N=.905
690          GOTO Calc
700      END IF
710      IF Re>4000 THEN
720          Kk=.174
730          N=.619
740          GOTO Calc
750      END IF
760      IF Re>40 THEN
770          Kk=.615
780          N=.466
790          GOTO Calc
800      END IF
810      IF Re>4 THEN
820          Kk=.021
830          N=.395
840          GOTO Calc
850      END IF
860      Kk=.091
870      N=.33
880  Calc:
890      H=(Kk*K/D)*(V*(D/100.)/Nu)^N
900      MOVE Vold,Hold
910      DRAW V,H
920      Vold=V
930      Hold=H
940  NEXT V
950  LINE TYPE 6
960  Vold=0
970  MOVE 0,0
980  Hold=0
1000  FOR V=1 TO 10
1010      Re=Row*V*(D/100.)/Mu
1020      IF Re<50 THEN
1030          Nud=.91*Pr^.31*Re^.395
1040      ELSE
1050          Nud=.6*Pr^.31*Re^.5
1060      END IF
1070      H=Nud*Correct*K/D
1080      H=Nud*K/D
1090      MOVE Vold,Hold
1100      DRAW V,H

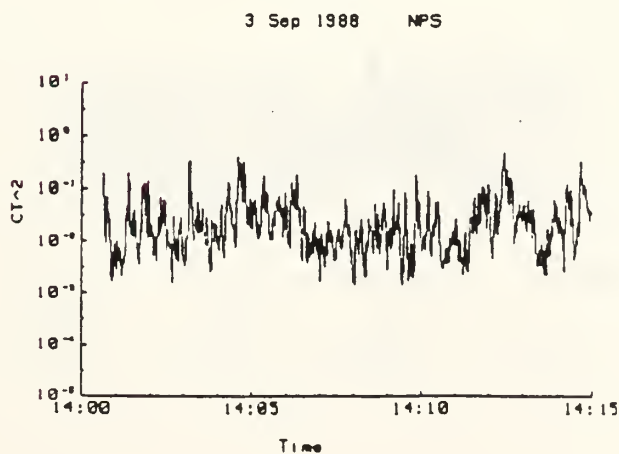
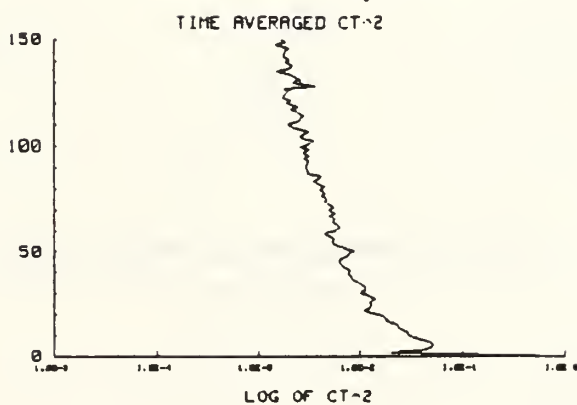
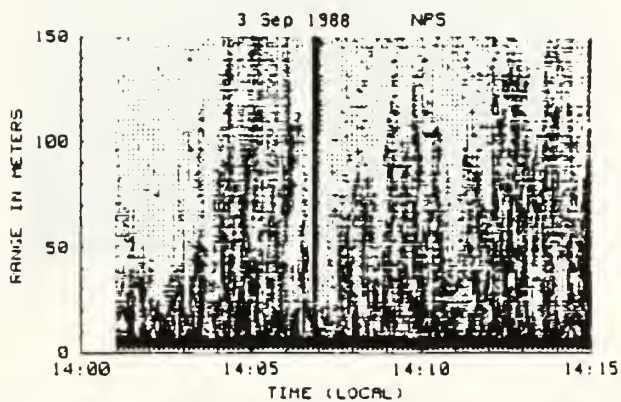
```

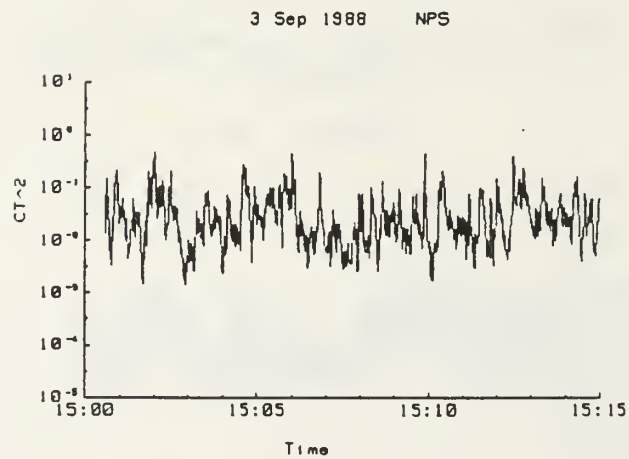
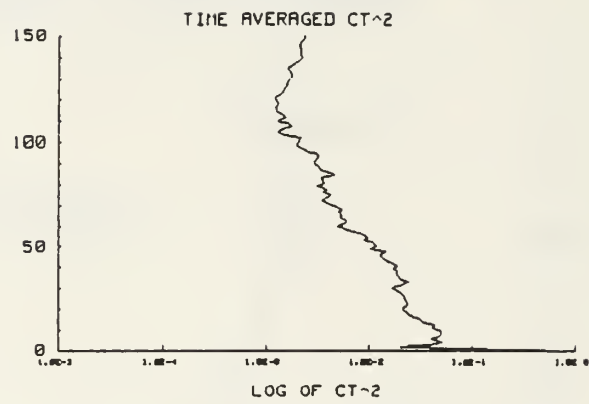
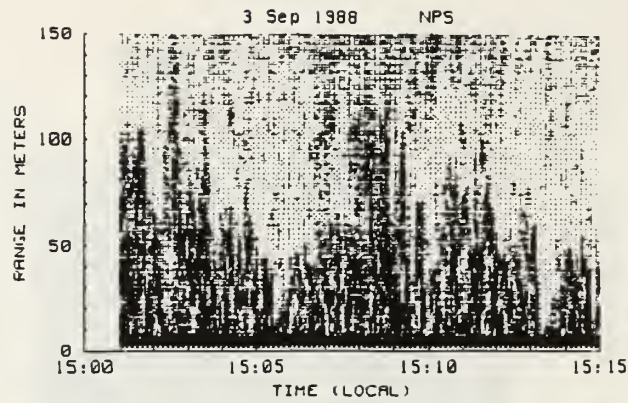
```

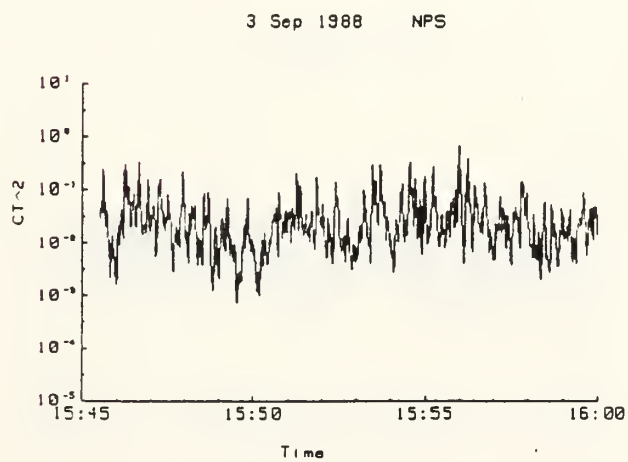
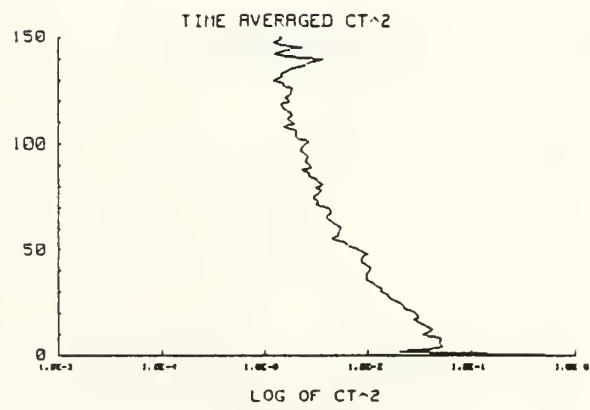
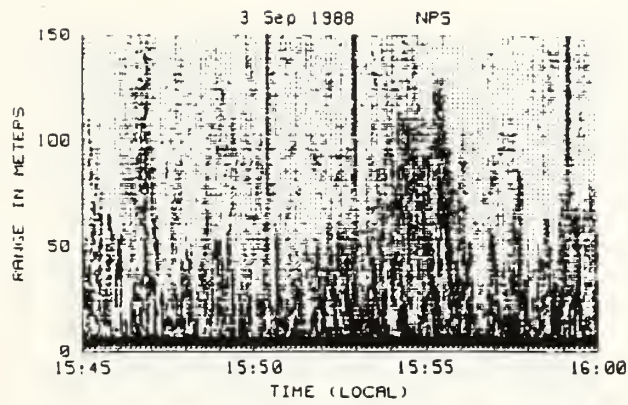
1120   Uold=U
1130   Hold=H
1140   NEXT U
1150   !
1160   CSIZE 3
1170   LINE TYPE 5
1180   MOVE 1,.55
1190   DRAW 2,.55
1200   MOVE 3,.55
1210   LINE TYPE 1
1220   LABEL " CAMPBELL(KRIETH)"
1230   LINE TYPE 5
1240   MOVE 5,.55
1250   DRAW 7,.55
1260   MOVE 9,.55
1270   LINE TYPE 1
1280   LABEL " AFGL(KRAMERS)"
1290   MOVE 0,0
1300   LINE TYPE 4
1310   FOR U=1 TO 5
1320     H=0.49255E-3/((.309375-((U-1)*.0307692))
1330     DRAW U,H
1340   NEXT U
1350   MOVE 3,.5
1360   DRAW 4,.5
1370   MOVE 5,.5
1380   LINE TYPE 1
1390   LABEL "EXPERIMENTAL"
1400   DUMP GRAPHICS #701
1450   END

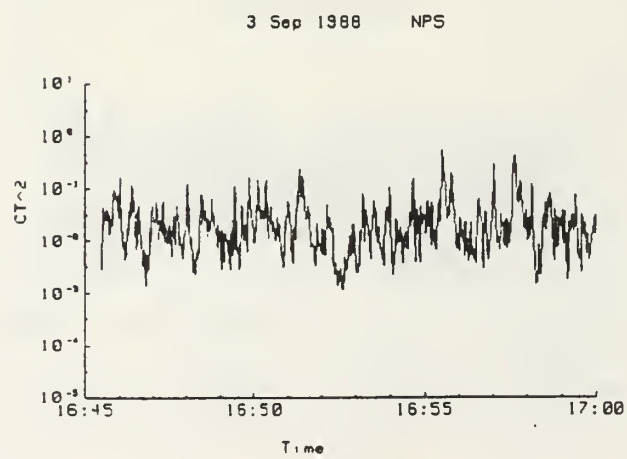
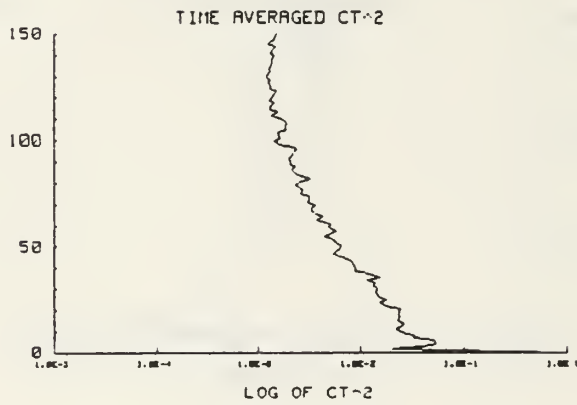
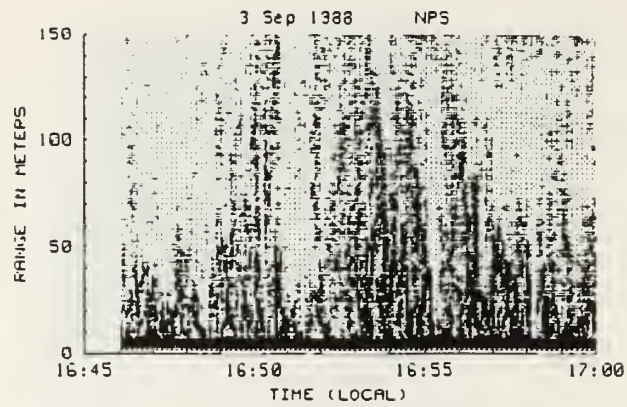
```

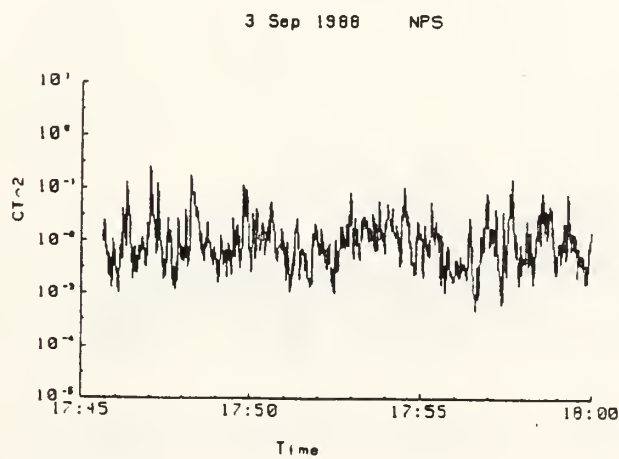
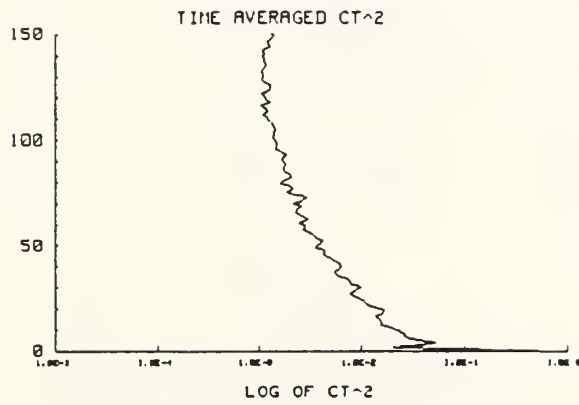
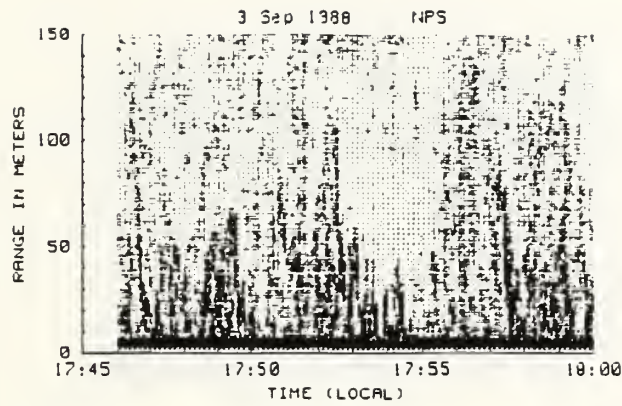
APPENDIX D **COMPARISON TEST DATA**

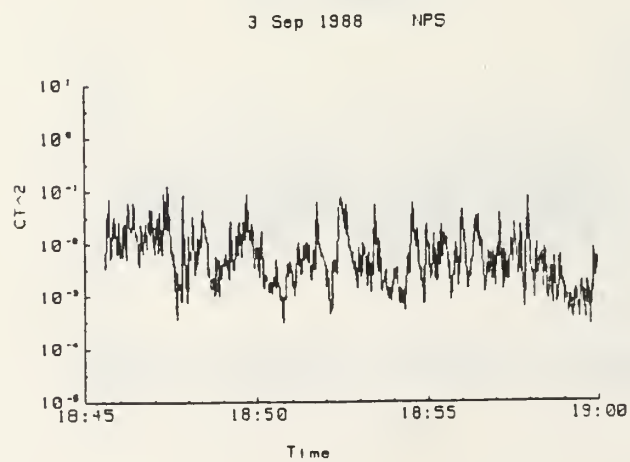
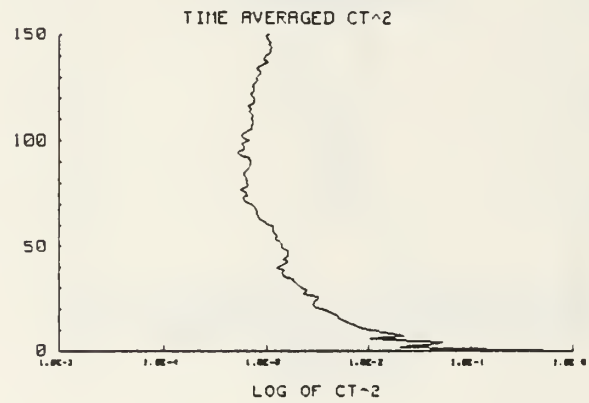
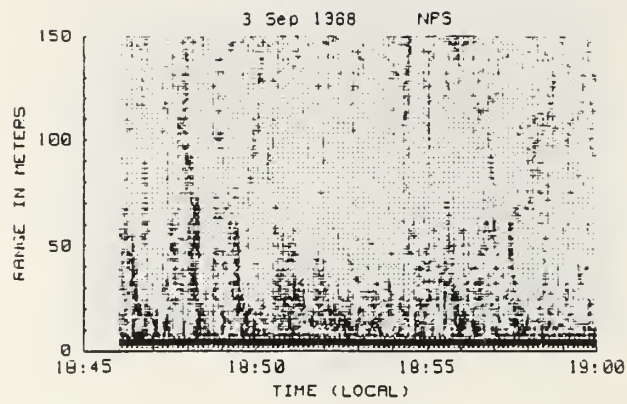


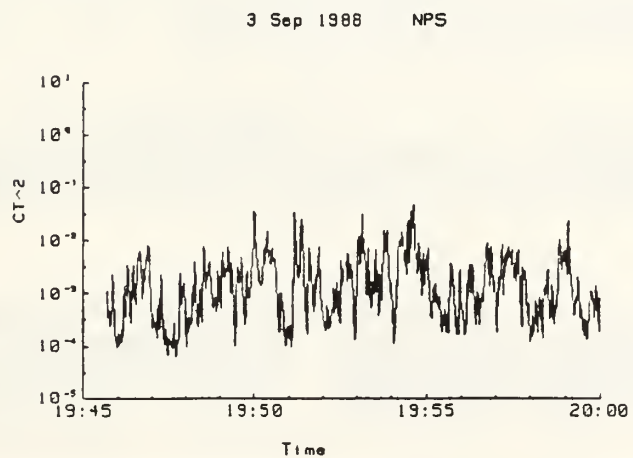
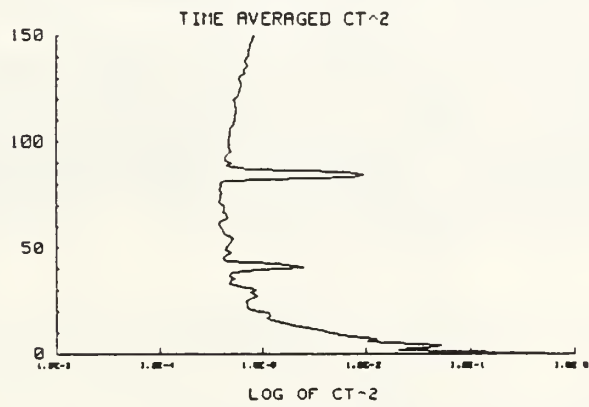
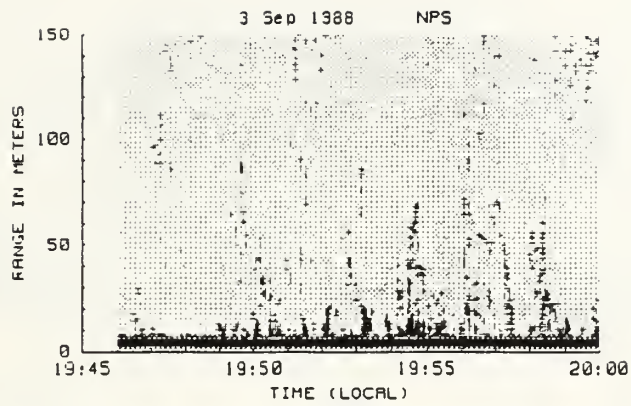












LIST OF REFERENCES

1. Bloemberge, N., Patel, C. K. N., et al., "The Science and Technology of Directed Energy Weapons," Reviews of Modern Physics, Vol. 59, No. 3, Part 2, Chapter 5, The American Physical Society, July 1987.
2. Good, R. E., et. al., Atmosphere Characterization at the HIDL Site CLEAR II Program, 26 February-9 March 1985, ASL-TR-0204, Atmospheric Sciences Laboratory, White Sands, New Mexico, 1985.
3. Walters, D. L., Favier, D. L., and Hines, J. R., "Vertical Path Atmospheric MTF Measurements," Journal of the Optical Society of America, Vol. 69, pp.828-837, 1979.
4. Stevens, K. B., Remote Measurement of the Atmospheric Isoplanatic Angle and Determination of Refractive Turbulence Profiles by Direct Inversion of the Scintillation Amplitude Covariance Function with Tikhonov Regularization, P.H.D. Dissertation, Naval Postgraduate School, Monterey, California, December 1985.
5. Walters, D. L. and Kunkel, K. E., "Atmospheric Modulation Transfer Function for Desert and Mountain Locations: The Atmospheric Effects of r_0 ," Journal of the Optical Society of America, Vol. 71, pp. 397-405, 1981.
6. Weingartner, F. J., Development of an Acoustic Echosounder for Detection of Lower Level Atmospheric Turbulence, M.S. Thesis, Naval Postgraduate School, Monterey, California, June 1987.
7. Brown, J. H., Good, R. E., Bench, P. M. and Faucher, G., Sonde Experiments for Comparative Measurements of Optical Turbulence, AFGL-TR-82-0079, Air Force Geophysics Laboratory, Hanscom AFB, Massachusetts, 1982.
8. Tatarski, V. I., Wave Propagation in a Turbulent Medium, Dover Publications, New York, 1961.
9. Fried, D. L., "Anisoplanatism in Adaptive Optics," Journal of the Optical Society of America, Vol. 72, pp. 52-61, 1982.

10. Clifford, S. F., "The Classical Theory of Wave Propagation in a Turbulent Medium," Topics in Applied Physics, Laser Beam Propagation in the Atmosphere, Vol. 25, Chapter 2, Springer-Verlag, 1978.
11. Kunkel, K. E. and Walters, D. L., "Behavior of the Temperature Structure Parameter in a Desert Basin," Journal of Applied Meteorology, Vol. 20, pp. 130-136, February 1981.
12. Wesely, M. L., "The Combined Effects of Temperature and Humidity Fluctuations on Refractive Index," Journal of Applied Meteorology, Vol. 15, pp. 43-49, January 1976.
13. Lawrence, R. S., Ochs, G. R. and Clifford, S. F., "Measurements of Atmospheric Turbulence Relevant to Optical Propagation," Journal of the Optical Society of America, Vol. 60, No. 6, pp. 826-830, June 1970.
14. Tennekes, H. and Lumley, J. L., A First Course in Turbulence, The M.I.T. Press, Cambridge, Massachusetts, 1972.
15. Gossard, E. E., "Finestructure of Elevated Stable Layers observed by Soudner and In Situ Tower Sensors," Journal of the Atmospheric Sciences, Vol. 42, No. 20, pp. 2156-2169, October 1985.
16. Kinzie, P. A., Thermocouple Temperature Measurement, John Wiley & Sons, New York, 1973.
17. Boerdijk, A. H., "Contributions to a General Theory of Thermocouples," Journal of Applied Physics, Vol. 30, No. 7, July 1959.
18. Linear Technologies Handbook, Linear Technologies Corporation, 1986.
19. Frederickson, T. C., Intuitive IC OP AMPS, National Semiconductor Technology Series, 1984.
20. OMEGA Temperature Handbook, OMEGA Engineering INC., 1988.
21. Perry, A. E., Hot-wire Anemometry, Clarendon Press, Oxford, 1982.

22. Kreith, F., Principles of Heat Transfer, International Textbook Company, Scranton, Pennsylvania, 1968.
23. Brown, J. H. and Good, R. E., Thermocouple and UHF Radar Measurements of C_n^2 at Westford Massachusetts-July 1981, AFGL-TR-84-0109, Air Force Geophysics Laboratory, Hanscom AFB, Massachusetts, 1984.
24. Campbell, G. S., Measurements of Air Temperature Fluctuations with Thermocouples, Atmospheric Science Laboratory, White Sands, New Mexico, 1969.
25. Kramers, H., "Heat Transfer from Spheres to Flowing Media," Physica, Vol. 12, No. 2, pp. 61-80, June 1946.
26. Cadet, D., "Energy Dissipation within Intermittent Clear Air Turbulence Patches," Journal of the Atmospheric Sciences, Vol. 34, pp. 137-142, January 1977.
27. Brown, J. H. and Beland, R. H., C_n^2 Measurements at AMOS, Air Force Geophysics Laboratory, Hanscom AFB, Massachusetts, March 1986.
28. Moxcey, L. R., Utilization of Dense Packed Planar Acoustic Echosounders to Identify Turbulence Structures in the Lowest Levels of the Atmosphere, M.S. Thesis, Naval Postgraduate School, Monterey, California, December 1987.
29. Ochs, G. R. and Hill, R. J., "Optical-Scintillation Method of Measuring Turbulence Inner Scale," Applied Optics, Vol. 24, No. 15, pp. 2430-2432, August 1985.
30. Hill, R. J. and Clifford, S. F., "Modified Spectrum of Atmospheric Temperature Fluctuations and its Application to Optical Propagation," J. Opt. Soc. AM., Vol. 68, No. 7, pp. 892-899, July 1978.

BIBLIOGRAPHY

Clark, J. A., Theory and Fundamental Research in Heat Transfer, The Macmillan Company, New York, 1963.

Elsasser, W. M., Heat Transfer by Infrared Radiation in the Atmosphere, Harvard University Printing Office, Cambridge, Massachusetts, 1942.

Feygel'son, Ye. M. and Tsvang, L. R., Heat Transfer in the Atmosphere, NASA TT f-790, National Aeronautics and Space Administration, Washington, DC, July 1974.

Jursa, A. S. ed., Handbook of Geophysics and the Space Environment, Air Force Geophysics Laboratory, Air Force Systems Command, 1985.

Lettau, H. H. and Davidson, B., Exploring the Atmosphere's First Mile, Vol. 1, Pergamon Press, New York, 1957.

Smol'yakov, A. V. and Tkachenko, V. M., The Measurement of Turbulent Fluctuations, Springer-Verlag, New York, 1983.

Wolfe, W. L. and Zissis, G. J. eds., The Infrared Handbook, Office of Naval Research, Washington, DC, 1978.

INITIAL DISTRIBUTION LIST

- | | |
|---|---|
| 1. Defense Technical Information Center
Cameron Station
Alexandria, VA 22304-6145 | 2 |
| 2. Library, Code 0142
Naval Postgraduate School
Monterey, CA 93943-5002 | 2 |
| 3. Prof. Donald L. Walters
Department of Physics (Code 61We)
Naval Postgraduate School
Monterey, CA 93943-5004 | 5 |
| 4. LT Michael Olmstead
531 Park Ave.
Laurel Springs NJ 08021 | 2 |
| 5. Space Defense Initiative Organization
SDIO/DE
1717 H Street
Washington, D.C. 20301 | 1 |
| 6. Research Administration Office
Code 012
Naval Postgraduate School
Monterey, CA 93943-5000 | 1 |
| 7. Kenneth J. Johnson
Code 4130
Naval Research Laboratory
Washington, D.C. 20375-5000 | 1 |

Thesis
0472 Olmstead
c.1 Development of a
differential temperature
probe for the measure-
ment of atmospheric tur-
bulence at all levels.

Thesis
0472 Olmstead
c.1 Development of a
differential temperature
probe for the measure-
ment of atmospheric tur-
bulence at all levels.



thesO472

Development of a differential temperatur



3 2768 000 82387 6

DUDLEY KNOX LIBRARY